Journal of Sound and Vibration (1999) **225**(5), 857–885
Article No. jsvi.1999.2277, available online at http://www.idealibrary.com on IDEAL®

SIMULTANEOUS PARAMETRIC AND INTERNAL RESONANCES IN SYSTEMS INVOLVING STRONG NON-LINEARITIES

R. A. IBRAHIM

Department of Mechanical Engineering, Wayne State University, Detroit, MI 48202, *USA*

AND

M. A. EL-SAYAD

Department of Engineering Mathematics, Alexandria University, Alexandria, Egypt

(*Received* 20 *August* 1998, *and in final form* 8 *March* 1999)

The non-linear dynamic interaction between the impact of the first asymmetric liquid sloshing mode, represented by an equivalent pendulum, and the elastic structural dynamics is examined in the neighborhood of simultaneous occurrence of parametric and internal resonance conditions. The analytical modelling of the impact force is described by a power function. The present work considers both weak and strong non-linear forces on interaction. The method of multiple scales is used to determine the system response in the neighborhood of three sets of different resonance conditions. Under first- or mixed-mode parametric excitation, the normal modes interact through internal resonance condition. The system response is found to be strongly dependent on initial conditions. Depending on the initial conditions and internal detuning parameter, the response can be quasi-periodic or chaotic with irregular jumps between two unstable equilibria. In the presence of impact forces, the system preserves fixed response amplitude response within a small range of internal detuning parameter. Beyond that range, the response exhibits quasi-periodic motion mainly governed by the initial conditions, internal detuning parameter, damping ratios and excitation level. Under second- mode parametric excitation, the second mode reaches fixed response, depending on initial conditions, with no energy sharing with the first mode. However, the phase angles are found to vary with time. Under combination parametric resonance, and in the absence of impact forces, the response is found to be sensitive to initial conditions.

1. INTRODUCTION

The linear modelling of parametric excited systems is quite adequate to predict the stability state of the equilibrium position. If the equilibrium is unstable, the linearized analysis will show an exponential growth of the response amplitude without limit. However, most real systems possess a non-linearity which becomes predominant such that when the response reaches a certain level, the system ends

0022-460X/99/350857 + 29 $30.00/0

up in a bounded limit cycle. In multi-degree-of-freedom systems, the equations of motion may be non-linearity coupled such that one mode may indirectly excite the other modes. Such non-linear modal interaction can be of considerable effect under certain conditions. This type of coupling is referred to an *autoparametric interaction* when an externally excited mode can act as a parametric excitation for further modes. In autonomous systems, a certain type of instability may occur when the normal mode frequencies are related by the relationship $\sum_{i=1}^{n} k_i\omega_i = 0$, where k_i are integers. This relationship is referred to as "internal resonance condition". The vector $\mathbf{k} = \{k_1, k_2, \ldots, k_n\}$ is called the resonance vector, while the number $k = |k_1| + |k_2| + \cdots + |k_n|$ is called the order of internal resonance. In the case of non-autonomous systems, a state of autoparametric resonance may occur when the contribution of internal resonance exists simultaneously with an external resonance as a result of external force.

The problem of internal resonances in non-linearly coupled oscillators is of much interest in connection with redistribution of energy among the various natural modes. This energy sharing is usually brought about by resonant interactions among the natural modes of the system. The nature of couplings among these modes plays a crucial role in such interactions. In a straightforward perturbation theory, internal resonances lead to the problem of small divisors which are associated with terms having factors such as $(\sum_{i=1}^{N} k_i\omega_i)^{-1}$.

In Hamiltonian autonomous systems, the simultaneous presence of several internal resonance relationships may result in some types of instability caused by certain non-linear terms in the system equations of motion. Stability analysis of such systems has been considered for different cases of internal resonance conditions [1–5]. Kunitsyn and Matveyev [4] formulated the normal form of a system that contains the first non-linear terms for an arbitrary number of non-interacting resonances of odd order. They classified the internal resonance conditions as weak and strong. Weak resonance preserves the stability of the system, while strong resonance results in system instability. However, the interaction of several weak internal resonances linked by more than one common frequency can result in system instability. The stability of the steady state responses of dynamic systems with multiple odd- and even-order internal resonances was considered by Kunitsyn and Markeev [6] and Kunitsyn and Perezhogin [7] respectively. These studies have shown that the problem of stability of systems with fourth order internal resonances is more complicated than for third order internal resonances. The stability of the equilibrium position of multi-dimensional Hamiltonian systems was determined for multiple independent and interacting resonance conditions. Interacting resonances imply that one or more frequencies are common in two internal resonance conditions. Kunitsyn and Tuyakbayev [8] found that if among resonance conditions there exists at least one strong resonance, then the trivial solution of the system is unstable. On the other hand, if all independent resonances are weak, then the trivial solution is stable [9]. Zhuravlev [10] considered different types of oscillation shapes in the configuration space and manifold space in the presence of multiple internal resonances. In the absence of perturbation, a subspace exists in which every trajectory is a closed curve. These trajectories become unstable under infinitesimally small perturbations.

When the non-linear system is subjected to an impulsive acceleration, the system may experience impact loading if it carries movable components such as liquids in partially filled containers, Methods for estimating the liquid impact and the associated pressure involved are not well developed. The only way to know the impact pressure have been reported through experimental studies. The sloshing impact loading cannot be viewed as a single loading event since it can be repeated due to the inertia and restoring forces. This type of impact is known in the literature as vibro-impact [11]. Systems involving vibro-impact with masses collide with rigid or elastic barriers during their oscillations and constitute a specific class of strongly non-linear systems. The non-linearity is mainly due to extremely rapid velocity changes during impacts. These changes are usually treated as being instantaneous (velocity jumps) and they lead to various strongly non-linear features of system behavior. If the system is linear with constant coefficients and is subjected to impact loading it will experience non-linear behavior. Hunt and Grossley [12] replaced the sudden change of the velocity during impact between colliding bodies by a strongly non-linear mass–spring–damper system. Vedenova *et al.* [13] replaced the impact forces by a high-power force which covers both elastic and rigid impact cases.

In the absence of internal resonances, the non-linear modal interaction of a pendulum, describing impact motion, with an elastic support structure was examined by Shaw and Shaw [14] and Pilipchuk and Ibrahim [15]. Shaw and Shaw represented the impact by the momentum equation together with the coefficient of restitution. They also assumed the collision between the pendulum mass and its barrier walls as a discontinuous process. One can also phenomenologically describe the interaction between the pendulum and the barrier with a special potential field, which is very weak in the region between the barrier walls and then becomes fast growing as it reaches the barrier walls [15]. Pilipchuk and Ibrahim found that the response behavior reveals that a high-frequency out-of-phase non-linear mode takes place with relatively small tank amplitude, and is more stable than the in-phase oscillation mode under small perturbations. The in-phase mode has relatively large tank amplitudes and does not preserve its symmetry under periodic parametric excitation. The work of Pilipchuk and Ibrahim was extended by El-Sayad *et al.* [16], who included non-linear coupling between the supporting structure and the pendulum motion. Under parametric excitation, El-Sayad *et al.* examined the system response under three different types of parametric resonance conditions. When the first mode was parametrically excited, the system exhibits hard non-linear behavior and the impact loading reduced the response amplitude. On the other hand, when the second mode was parametrically excited, the impact loading results in complex response behavior characterized by multiple steady state solutions, where the response switches from soft to hard non-linear characteristics. Under combination parametric resonance of summed type, the system possesses a single steady state response in the absence and in the presence of impact. However, the system response followed a soft behavior in the absence of impact and switches to a hard one in the presence of impact.

The purpose of the present work is to examine the dynamic response characteristics under simultaneous occurrence of internal and parametric resonances in the presence of impact forces. The method of multiple scales (see, for

example, reference [17]) is used and the impact forces are described by quintic power non-linearity. Basically, the system response will be examined under the following set of resonance conditions: (1) $\omega_2 = 3\omega_1$ and $\Omega_y = 2\omega_1$, (2) $\omega_2 = 3\omega_1$ and $\Omega_y = 2\omega_2$, and (3) $\omega_2 = 3\omega_1$ and $\Omega_y = \omega_1 + \omega_2$, where ω_1, ω_2 are the normal mode frequencies of the system and Ω_y is the parametric excitation frequency. The reason for selecting these three resonance conditions is due to the fact that each set will provide different dynamic characteristics.

2. EQUATIONS OF MOTION

Consider a liquid container supported by four massless rods of length L, which are restrained by four torsional springs of stiffness k at the base as shown in Figure 1. The base is subjected to vertical base acceleration $F_y(t)$. Let M be the total mass of the container including liquid and m the equivalent sloshing mass of the first asymmetric mode of the liquid. The fluid-free surface is modelled as a pendulum of length l. The equivalent pendulum parameters for different types of container geometry are well documented in Abramson [18]. The pendulum can reach the walls of the tank if its angle with the vertical axis is $\theta = \pm \theta_0$. One can phenomenologically describe the interaction between the pendulum and the tank walls with a power function [15], $F_{\text{impact}} = b(\theta/\theta_0)^{2n-1}$, where $n \gg 1$ in an integer and b is a positive constant parameter usually measured experimentally. One has a limit of absolutely rigid bodies' interaction, if $n \to \infty$. A finite value of n seems more realistic than the rigid-body limit, yet the approach includes the rigid-body limit as a particular case. The interaction between the pendulum and the tank walls

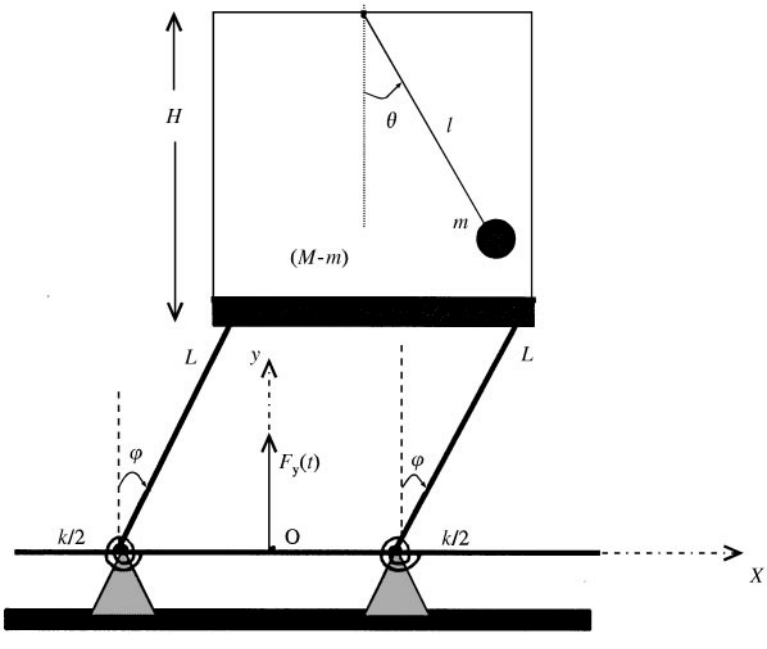

Figure 1. Schematic diagram of the model.

is very weak in the region $|\theta| < \pm\theta_0$, but becomes fast growing in the neighborhood of the points $|\theta| = \pm\theta_0$. The localized dissipative force will be approximated by the expression $F_d = d(\theta/\theta_0)^{2p}\dot{\theta}$, where d is a constant, p is a positive integer (generally $p \neq n$) and a dot denotes differentiation with respect to time t.

Using Lagrange's equation with respect to the co-ordinates θ and φ, and introducing the approximation $\sin\theta \approx \theta - \theta^3/3!$ and $\cos\theta \approx 1 - \theta^2/2$, the equations of motion are

$$\ddot{\theta} + \frac{g}{l}\theta - \frac{L}{l}\ddot{\varphi} = \frac{L}{2l}\ddot{\varphi}(\theta+\varphi)^2 + \frac{L}{l}\dot{\varphi}^2(\theta+\varphi) + \frac{F_y(t)}{l}\theta + \frac{g}{6l}\theta^3 - \frac{d}{ml^2}\left(\frac{\theta}{\theta_0}\right)^{2p}\dot{\theta} - \frac{b}{ml^2}\left(\frac{\theta}{\theta_0}\right)^{2n-1}, \tag{1}$$

$$\ddot{\varphi} + \left(\frac{k}{ML^2} - \frac{g}{L}\right)\varphi + \frac{ml}{ML}\ddot{\theta} = \frac{ml}{2ML}\ddot{\theta}(\theta+\varphi)^2 + \frac{ml}{ML}(\theta+\varphi)\dot{\theta}^2 - \frac{g}{6L}\varphi^3 - \frac{F_y(t)}{L}\varphi. \tag{2}$$

Introducing the non-dimensional parameters

$$\Theta = \theta/\theta_0, \quad \Phi = \varphi/\theta_0, \quad \tau = \omega_l t, \quad \omega_l^2 = g/l, \quad \omega_L^2 = (k/ML^2) - g/L,$$
$$\nu = \omega_l/\omega_L, \quad \mu = \mu/M, \quad \lambda = l/L, \quad f_y(\tau) = F_y(\tau/\omega_l)/l\omega_l^2\theta_0 \tag{3}$$

gives

$$\begin{pmatrix} 1 & \frac{1}{\lambda} \\ \mu\lambda & 1 \end{pmatrix}\begin{Bmatrix} \Theta'' \\ \Phi'' \end{Bmatrix} + \begin{bmatrix} \mu\lambda^2 & 0 \\ 0 & \nu^2 \end{bmatrix}\begin{Bmatrix} \Theta \\ \Phi \end{Bmatrix} = \begin{Bmatrix} \mu\lambda^2 Q_{11} \\ Q_{22} \end{Bmatrix}, \tag{4}$$

where a prime denotes differentiation with respect to τ. Q_{ii} stands for non-linear and excitation terms. Equations (4) are linearly coupled through the mass matrix. They are also non-linearly coupled through inertia non-linearity. The coefficients b and d, and the exponents n and p are usually obtained experimentally. However, in the absence of experimental data, one may select $n = 3$ and $p = 2$, while the influence of the coefficients b and d will be examined in the present work. Both co-ordinates are parametrically excited. Higher-order exponents can be selected but will result in more lengthy analysis. Any possible solution for equations (4) gives the total motion as a sum of responses in its characteristic modes of vibration. In order to derive the solution in terms of these principal modes, a transformation to the principal co-ordinates $\mathbf{Y}$ should be carried out. Introducing the linear transformation into equations (4),

$$\begin{Bmatrix} \Theta \\ \Phi \end{Bmatrix} = [P]\begin{Bmatrix} Y_1 \\ Y_2 \end{Bmatrix} = \begin{bmatrix} 1 & 1 \\ K_1 & K_2 \end{bmatrix}\begin{Bmatrix} Y_1 \\ Y_2 \end{Bmatrix}, \tag{5}$$

where $[P]$ is the modal matrix with $K_{1,2} = \lambda(1 - \omega_{1,2}^2)/\omega_{1,2}^2$ and $\omega_{1,2}^2 = [(1+\nu^2) \mp \sqrt{(1-\nu^2)^2 + 4\mu\nu^2}]/[2(1-\mu]$. Now pre-multiplying equation (4) by

$[P]^{\mathrm{T}}$, where T denotes transpose, gives

$$Y_1'' + \omega_1^2 Y_1 = \varepsilon\{-2\bar{\zeta}_1\omega_1 Y_1' + (\Psi_{11})_{gn} + (\Psi_{11})_{impact} + (\Psi_{11})_{ex}\}, \tag{6a}$$

$$Y_2'' + \omega_2^2 Y_2 = \varepsilon\frac{m_{11}}{m_{22}}\{-2\bar{\zeta}_2\omega_2 Y_2' + (\Psi_{22})_{gn} + (\Psi_{22})_{impact} + (\Psi_{22})_{ex}\}, \tag{6b}$$

where linear viscous damping $\zeta_i = \varepsilon\bar{\zeta}_i$, with $\varepsilon = \mu\lambda^2/m_{11}$, has been introduced to account for energy dissipation, ω_i are the normal mode frequencies and m_{ii} are constant coefficients. The right-hand sides of these equations include inertia and stiffness non-linearities of cubic order and are denoted by subscript "gn". They also include impact non-linearities of quintic order and are denoted by subscript "impact". The subscript "ex" stands for excitation terms. The impact and geometric non-linear terms are treated of the same order of $O(\varepsilon)$ since the coefficients of the impact terms are of higher order of magnitude than those coefficients of cubic terms. The functions Ψ_{ii} are listed in Appendix A.

3. SYSTEM RESPONSE ANALYSIS

In order to identify the critical non-linear resonance conditions and to solve for the system response in the neighborhood of these conditions, the multiple scales method will be used. The solution of equations (6) may be expressed in a uniform expansion form [17]

$$Y_i = Y_{i0}(T_0, T_1, T_2, \dots) + \varepsilon Y_{i1}(T_0, T_1, T_2, \dots) + \cdots, \tag{7}$$

where $T_0 = \tau T_1 = \varepsilon\tau$, $T_2 = \varepsilon^2\tau, \dots$ i.e. $T_n = \varepsilon^n\tau$, $n = 0,1,2, \dots$.
Using the chain rule, we write

$$\frac{\mathrm{d}}{\mathrm{d}t} = \frac{\partial}{\partial T_0} + \varepsilon\frac{\partial}{\partial T_1} + \varepsilon^2\frac{\partial}{\partial T_2} + \cdots = D_0 + \varepsilon D_1 + \varepsilon^2 D_2 + \cdots, \quad D_n = \frac{\partial}{\partial T_n},$$

$$\frac{\mathrm{d}^2}{\mathrm{d}t^2} = D_0^2 + 2\varepsilon D_0 D_1 + \varepsilon^2(D_1^2 + 2D_0 D_2) + \cdots. \tag{8}$$

The expansion is carried out up to first-order in ε. Accordingly, we need to deal with the two time scales T_0 and T_1. Substituting the solution (7) into equations (6) using the transformed time derivatives (8) gives

$$(D_0^2 + 2\varepsilon D_0 D_1 + \varepsilon^2(D_1^2 + 2D_0 D_2) + \cdots)Y_i + \omega_i^2 Y_i = \varepsilon\Psi_i. \tag{9}$$

Equating the coefficients of equal powers of ε^0 and ε^1 (ε^n) gives a set of differential equations to be solved for Y_{i0} and Y_{i1}. For equation (6a) the zero and first order equations in ε are, respectively,

$$D_0^2 Y_{10} + \omega_1^2 Y_{10} = 0, \tag{10}$$

$$D_0^2 Y_{11} + \omega_1^2 Y_{11} = -2D_0 D_1 Y_{10} - 2\bar{\zeta}_1\omega_1 D_0 Y_{10} + \Pi_{11}(Y_{ij}) \tag{11}$$

For equation (6b) the zero and first order equations in ε are, respectively,

$$D_0^2 Y_{20} + \omega_2^2 Y_{20} = 0, \tag{12}$$

$$D_0^2 Y_{21} + \omega_2^2 Y_{21} = -2D_0 D_1 Y_{20} - 2\bar{\zeta}_2 \omega_2 D_0 Y_{20} + \Pi_{22}(Y_{ij}), \tag{13}$$

where Π_{ii} stands for non-linear, damping, and excitation terms. The general solutions of equations (10) and (12) can be written in the form

$$Y_{10} = A(T_1)\exp(\mathrm{i}\omega_1 T_0) + \bar{A}(T_1)\exp(-\mathrm{i}\omega_1 T_0), \tag{14}$$

$$Y_{20} = B(T_1)\exp(\mathrm{i}\omega_2 T_0) + \bar{B}(T_1)\exp(-\mathrm{i}\omega_2 T_0), \tag{15}$$

where an overbar denotes conjugate and $\mathrm{i} = \sqrt{-1}$. $A(T_1)$ and $B(T_1)$ are functions of the time scale T_1 and will de determined later. Substituting solutions (14) and (15) into equations (11) and (13) gives

$$D_0^2 Y_{11} + \omega_1^2 Y_{11} = -2D_0 D_1 \{A(T_1)\exp(\mathrm{i}\omega_1 T_0) + \bar{A}(T_1)\exp(-\mathrm{i}\omega_1 T_0)\} + \Psi_{11}(Y_{ij}) - 2\mathrm{i}\omega_1^2 \bar{\zeta}_1 (A(T_1)\exp(\mathrm{i}\omega_1 T_0) + \cdots, \tag{16}$$

$$D_0^2 Y_{21} + \omega_2^2 Y_{21} = -2D_0 D_1 \{B(T_1)\exp(\mathrm{i}\omega_2 T_0) + \bar{B}(T_1)\exp(-\mathrm{i}\omega_2 T_0)\} + \frac{m_{11}}{m_{22}} \Psi_{22}(Y_{ij}) - 2\mathrm{i}\omega_2^2 \bar{\zeta}_2 (B(T_1)\exp(\mathrm{i}\omega_2 T_0) + \cdots . \tag{17}$$

The right-hand sides of these equations contain terms that produce secular terms in Y_{i1}. In view of the system non-linearities and excitation, these secular terms establish different types of resonance conditions. Under parametric excitation, two types of resonance conditions may arise. These are (a) internal resonance condition of fourth order $\omega_2 = 3\omega_1$, and (b) parametric resonance conditions: (1) principal parametric resonance of the first mode $\Omega_y = 2\omega_1$, (2) principal parametric resonance of the second mode $\Omega_y = 2\omega_2$, (3) combination parametric resonance of the summed type $\Omega_y = \omega_1 + \omega_2$.

The response characteristics corresponding to simultaneous occurrence of the internal resonance condition (a) and one parametric resonance condition will be considered in the next three subsections. In each case, the solutions for the complex amplitudes A and B will be expressed in the complex polar form

$$A = \frac{a}{2}\exp(\mathrm{i}\alpha), \qquad B = \frac{b}{2}\exp(\mathrm{i}\beta). \tag{18}$$

3.1. FIRST MODE PARAMETRIC EXCITATION

Introducing the detuning parameters σ_y and σ_I defined by

$$\Omega_y = 2\omega_1 + \varepsilon\sigma_y \quad \text{and} \quad \omega_2 = 3\omega_1 - \varepsilon\sigma_I$$

and following the standard procedure of multiple scales gives the following set of first-order differential equations in the amplitudes a and b and the new phase angles $\gamma_1 = \sigma_y T_1 - 2\alpha$, and $\gamma_2 = \sigma_I T_1 - \beta + 3\alpha$:

$$\frac{\partial \gamma_1}{\partial T_1} = \sigma_y + \frac{2}{\omega_1}\left\{G_{13}\frac{Y_0}{4}\sin\gamma_1 + \bar{G}_2 a^2 + \bar{G}_1 b^2 + \left(\frac{G_{118}\omega_2}{8}\sin\gamma_2 + \bar{G}_6\ \cos\gamma_2\right)ab\right.$$

$$+ \frac{5}{16}C_{16}a^4 + \frac{15}{8}C_{16}b^4 - \bar{G}_4 a^2 b^2 - \bar{G}_7 ab^3\sin\gamma_2$$

$$\left. - \frac{3}{16}C_{15}(2\omega_1\sin\gamma_2 - 5\omega_2\cos\gamma_2)a^3 b\right\}, \tag{19}$$

$$\omega_1\frac{\partial \mathrm{a}}{\partial T_1} = -\frac{G_{13}}{4}\,Y_0 a\cos\gamma_1 - \omega_1^2\bar{\zeta}_1 a + \left(\bar{G}_6\sin\gamma_2 + \frac{G_{118}\omega_2}{8}\cos\gamma_2\right)a^2 b + \frac{\omega_1}{16}C_{15}a^5$$

$$-\frac{3}{8}\omega_1 C_{15}\mathrm{a}^4 b\cos\gamma_2 + \frac{3\omega_1}{8}\,C_{15}a^3 b^2$$

$$-\left(\bar{G}_7\cos\gamma_2 + \frac{15\omega_2}{16}\,C_{15}\sin\gamma_2\right)a^2 b^3 + \bar{G}_3 ab^4, \tag{20}$$

$$\frac{\partial \gamma_2}{\partial T_1} = \sigma_I - \frac{3}{4}\frac{G_{13}}{\omega_1}\,Y_0\sin\gamma_1 - \left(3\frac{\bar{G}_1}{\omega_1} + \frac{\bar{G}_9}{\omega_2}\right)b^2 - \left(3\frac{\bar{G}_2}{\omega_1} - \frac{\bar{G}_8}{\omega_2}\right)a^2 + \frac{\bar{G}_{11}}{\omega_2}\frac{a^3}{b}\cos\gamma_2$$

$$-\frac{3}{\omega_1}\left(\frac{G_{118}\omega_2}{8}\sin\gamma_2 + \bar{G}_6\cos\gamma_2\right)ab - \frac{15}{16}C_{16}\left(\frac{1}{\omega_1} - \frac{1}{\omega_2}\right)a^4$$

$$+\left(\frac{9}{8}C_{15} + \frac{\bar{G}_{12}}{\omega_2}\right)a^3 b\sin\gamma_2 + \left(3\frac{\bar{G}_4}{\omega_1} + \frac{\bar{G}_{10}}{\omega_2}\right)a^2 b^2$$

$$+\frac{3}{\omega_1}\left(\bar{G}_7\sin\gamma_2 - \frac{15}{16}\,C_{15}\omega_2\cos\gamma_2\right)ab^3 - \frac{5}{8}C_{16}\left(\frac{9}{\omega_1} - \frac{1}{2\omega_2}\right)b^4$$

$$+\frac{1}{32\omega_2}(\omega_1 C_{15}\sin_2 + 5C_{16}\cos\gamma_2)\frac{a^5}{b}, \tag{21}$$

$$\omega_2\frac{\partial b}{\partial T_1} = -\omega_2^2\bar{\zeta}_2 b - \bar{G}_{11}a^3\sin\gamma_2 + \frac{3\omega_1}{16}\,C_{15}a^4 b + \frac{\omega_2}{16}\,C_{15}b^5$$

$$+\bar{G}_{12}a^3 b^2\cos\gamma_2 + \frac{1}{32}C_{15}(\omega_1\cos\gamma_2 - 5\sin\gamma_2)a^5. \tag{22}$$

These equations are integrated numerically for mass ratio $\mu = 0{\cdot}2$, length ratio $\lambda = 0{\cdot}2$, local frequency ratio $\nu = 0{\cdot}5$, excitation amplitude ratio $Y_0 = 0{\cdot}1$, $C_{16} = -0{\cdot}5$, $C_{15} = -0{\cdot}05$ and damping ratios $\zeta_1 = \zeta_2 = 0{\cdot}1$. It is found that a stationary fixed solution cannot be obtained by setting the left-hand side to zero.

In the absence of impact, the response is examined by dropping the fifth order terms from equations (19)–(22). In this case, the amplitude and phase equations take the form

$$\frac{\partial \gamma_1}{\partial T_1} = \sigma_y + \frac{2}{\omega}\left\{G_{13}\frac{Y_0}{4}\sin\gamma_1 + \bar{G}_1 b^2 + \bar{G}_2 a^2 + \left(\frac{G_{118}\omega_2}{8}\sin\gamma_2 + \bar{G}_6\cos\gamma_2\right)ab\right\}, \tag{23}$$

$$\omega_1\frac{\partial a}{\partial T_1} = -G_{13}\,a\,\frac{Y_0}{4}\cos\gamma_1 - \omega_1^2\bar{\zeta}_1 a + \frac{G_{118}\omega_2}{8}a^2 b\cos\gamma_2, \tag{24}$$

$$\frac{\partial \gamma_2}{\partial T_1} = \sigma_I - \frac{3}{\omega_1}\left\{G_{13}\frac{Y_0}{4}\sin\gamma_1 + \frac{G_{118}\omega_2}{8}ab\sin\gamma_2 + \bar{G}_6\,ab\cos\gamma_2\right\} - \left(3\frac{\bar{G}_2}{\omega_1} - \frac{\bar{G}_6}{\omega_2}\right)a^2 - \left(3\frac{\bar{G}_1}{\omega_1} + \frac{\bar{G}_9}{\omega_2}\right)b^2 + \frac{\bar{G}_{11}}{\omega_2}\frac{a^3}{b}\cos\gamma_2, \tag{25}$$

$$\omega_2\frac{\partial b}{\partial T_1} = -\omega_2^2\bar{\zeta}_2 b - \bar{G}_{11}a^3\sin\gamma_2 \tag{26}$$

These equations belong to a non-integrable non-conservative class. Accordingly, one expects to observe complex response characteristics. It is found that in the presence of internal resonance the system responds in different ways depending on the internal detuning only at zero parametric detuning parameter. Figure 2 shows a sample of time history records for $\sigma_y = 0$ and $\sigma_I = 0$. The first mode oscillates about a mean value $\langle a\rangle \approx 0{\cdot}2$ while the second mode fluctuates with occasional spikes about its zero equilibrium position $b = 0$. Figure 3 shows the unimodal amplitude–frequency response (in the absence of internal resonance taken from reference [16]) including one point in the presence of internal resonance at $\sigma_y = 0$ with $\sigma_I = 0$. Obviously, the first-mode amplitude fluctuates around the unimodal parametric response. These fluctuations arise mainly due to internal resonance where there is an irregular energy distributional between the two modes.

If the internal detuning parameter is selected to be well remote from the exact internal resonance, the response may or may not achieve a steady state depending on initial conditions. For example, when $\sigma_I = -25$, Figure 4 shows that the system response is chaotic, where the first mode oscillates about its unimodal parametric response value, and the second mode oscillates about its zero equilibrium value. If the initial conditions are selected very small, such as $a = b = 0{\cdot}01$, the response amplitudes achieve fixed values $a = 0{\cdot}22$ and $b = 0{\cdot}1$.. The second-mode frequency spectrum is essentially wide band. As the internal detuning parameter σ_I increases, the response becomes quasi-periodic. Numerical integration has revealed that within the range of $\sigma_I = 6$–17, the response exhibits periodic solutions. This regime also oscillates about the unimodal response fixed point (as determined by the first-mode parametric excitation in the absence of internal resonance). There are regions of internal deturing parameters within the ranges $\sigma_I = -20$ through $+6$, and 18 through 55 where the response looks random in behavior. Over these regions, the first mode involves few frequency components while the second mode has a wide frequency spectrum with several spikes. Furthermore, the second mode

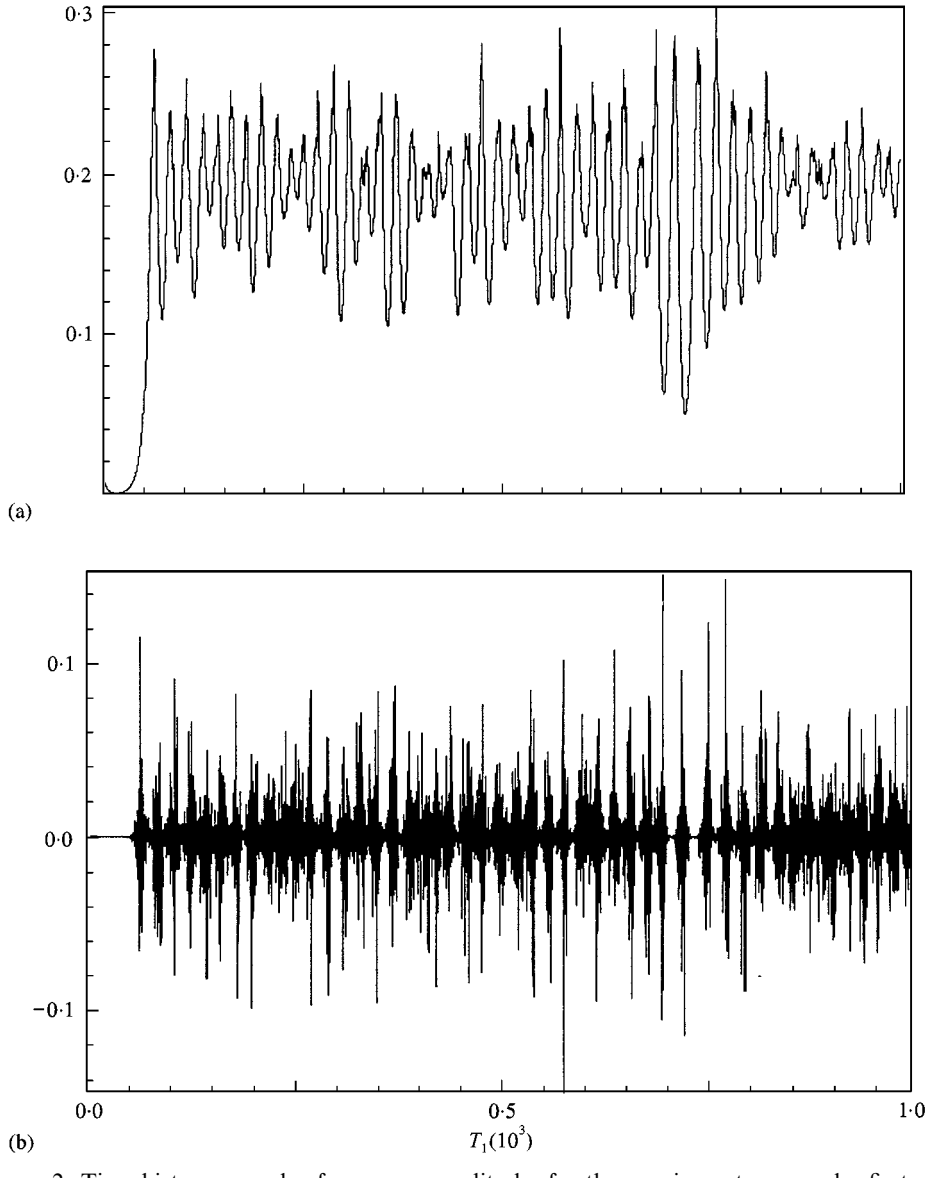

Figure 2. Time history records of response amplitudes for the non-impact case under first-mode parametric excitation for $Y_0 = 0{\cdot}2$, $\mu = 0{\cdot}2$, $\lambda = 0{\cdot}2$, $\sigma_y = 0{\cdot}0$, $\sigma_I = 0{\cdot}0$, $\zeta_1 = \zeta_2 = 0{\cdot}1$, and initial conditions (a) $(T_1 = 0) = 0{\cdot}01$, (b) $(T_1 = 0) = 0{\cdot}01$.

may or may not oscillate about its zero equilibrium position depending on the initial conditions. Figures 2 and 4 reveal that there are occasional symmetric spikes indicating that the response processes are essentially non-Gaussian with zero skewness and kurtosis greater than 3. The skewness is a statistical parameter measuring the asymmetry of the process and is expressed in terms of third order statistical moments. The kurtosis, on the other hand, measures the degree of flatness of the probability density curve about the mean value. The kurtosis is usually expressed in terms of the fourth-order moment.

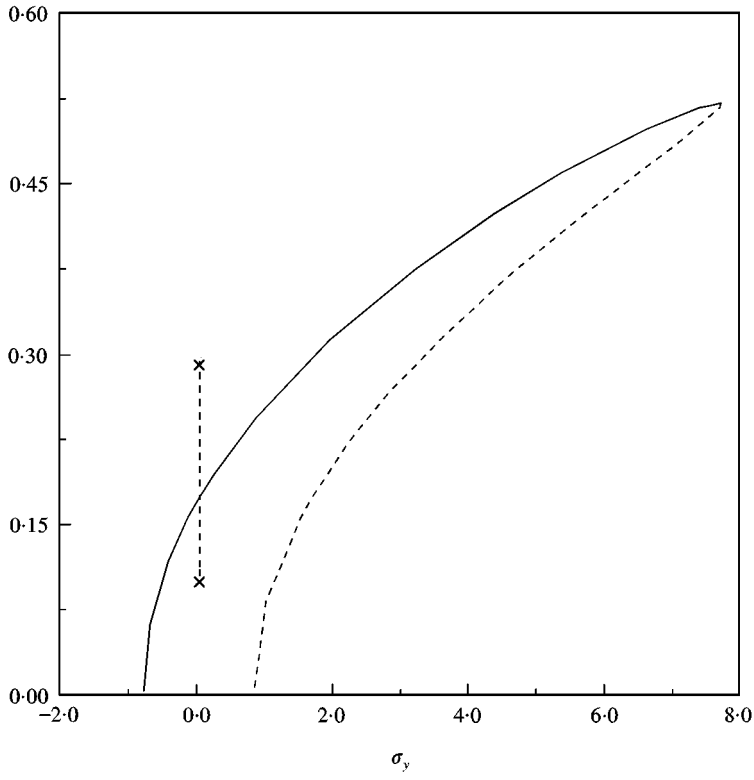

Figure 3. First-mode amplitude–frequency response curve in the absence of internal resonance [16] showing the response amplitude (dashed vertical line between two crosses) at $\sigma_y = 0{\cdot}0$ when the system is internally tuned for $\sigma_I = 0{\cdot}0$, $Y_0 = 0{\cdot}2$, $\mu = 0{\cdot}2$, $\lambda = 0{\cdot}2$, $\zeta_1 = \zeta_2 = 0{\cdot}1$.

For the impact case, the quintic terms should be included and equation (19)–(22) should be considered. The numerical integration yields non-stationary solutions in the form of chaotic motion as shown in Figure 5 for $\sigma_I = 0{\cdot}0$. Comparing Figure 5 with Figure 2 reveals that the impact loading results in asymmetry in the second-mode response indicating non-zero skewness. The second mode experiences wide frequency spectrum and involves several spikes in both the time and frequency domains. The unimodal amplitude–frequency response under parametric excitation is shown by solid and dashed curves in Figure 6 (taken from reference [16]). Figure 6 also includes the first-mode amplitude response in the presence of internal resonance $\sigma_I = 0{\cdot}0$ and indicated by the vertical dashed line at $\sigma_y = 0$. If the initial conditions are changed, the response takes completely different scenario characterized by large asymmetric spikes on the positive side of the response amplitude. The spike in the time domain of the second-mode response are found to persist as the detuning parameter increases.

More numerical integration revealed that within the internal detuning parameter range $\sigma_I = -15$ through -10, the response is found to be quasi-periodic. The response amplitudes always oscillate about non-zero mean values as shown in Figure 7. For internal detuning $\sigma_I > -10$ the response is chaotic with a wide frequency spectrum in the second-mode response.

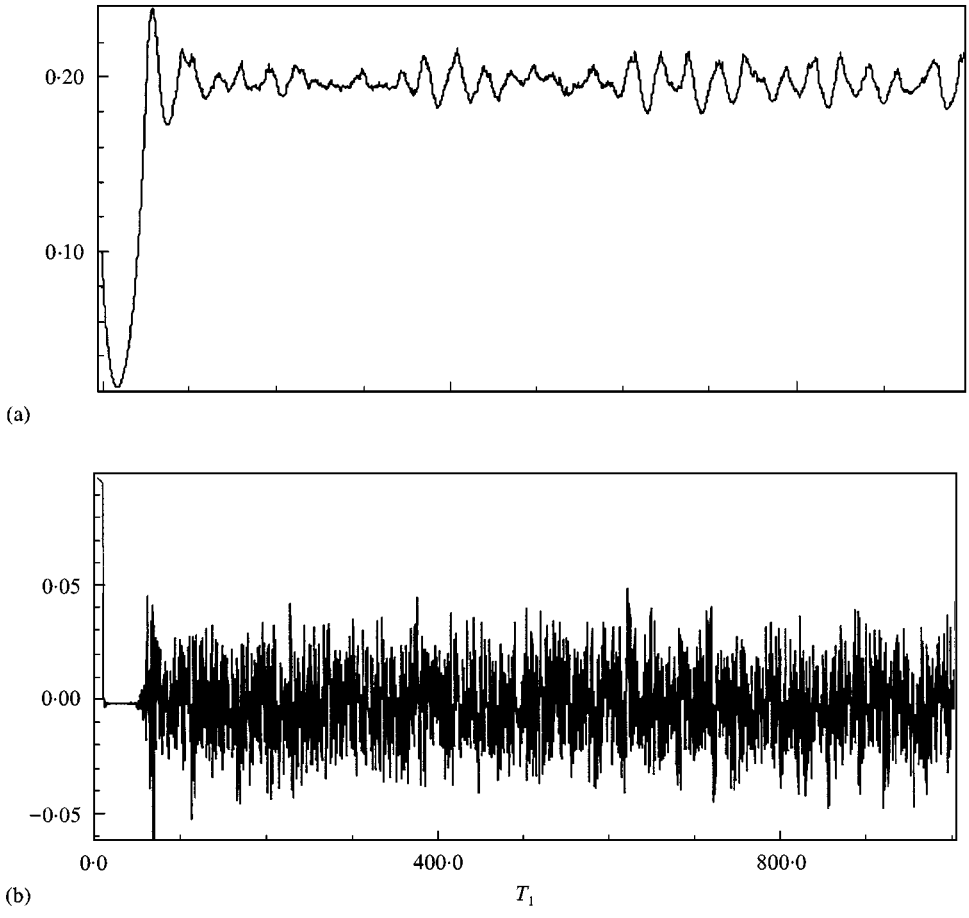

Figure 4. Time history records of response amplitudes for the non-impact case under first-mode parametric excitation for $Y_0 = 0{\cdot}2$, $\mu = 0{\cdot}2$, $\lambda = 0{\cdot}2$, $\sigma_y = 0{\cdot}0$, $\sigma_I = -25$, $\zeta_1 = \zeta_2 = 0{\cdot}1$, and initial conditions (a) $(T_1 = 0) = 0{\cdot}1$, (*b*) $(T_1 = 0) = 0{\cdot}1$.

3.2. SECOND-MODE PARAMETRIC EXCITATION

Introducing the detuning parameters σ_i such that $\Omega_1 = 2\omega_1 + \varepsilon\sigma_y$, and $\omega_2 T_0 = 3\omega_1 T_0 - \sigma_I T_1$ and the new phase angle γ defined by $\gamma_1 = \sigma_y T_1 - 2\beta$, and $\gamma_2 = \sigma_1 T_1 - \beta + 3\alpha$, the following first-order differential equations are obtained:

$$\frac{\partial\gamma_1}{\partial T_1} = \sigma_y + \frac{2}{\omega_2}\left\{G_{22}\frac{Y_0}{4}\sin\gamma_1 + (\bar{G}_6 + \bar{G}_8)a^2 + \bar{G}_9 b^2 + \bar{G}_{10}a^2b^2 + \bar{G}_{11}\frac{a^3}{b}\cos\gamma_2 + \frac{15}{16}C_{16}a^4 + \frac{5}{16}C_{16}b^4 + \bar{G}_{12}a^3 b\sin\gamma_2 + \frac{1}{32}\frac{a^5}{b}(\omega_1 C_{15}\sin\gamma_2 + 5C_{16}\cos\gamma_2)\right\}, \tag{27}$$

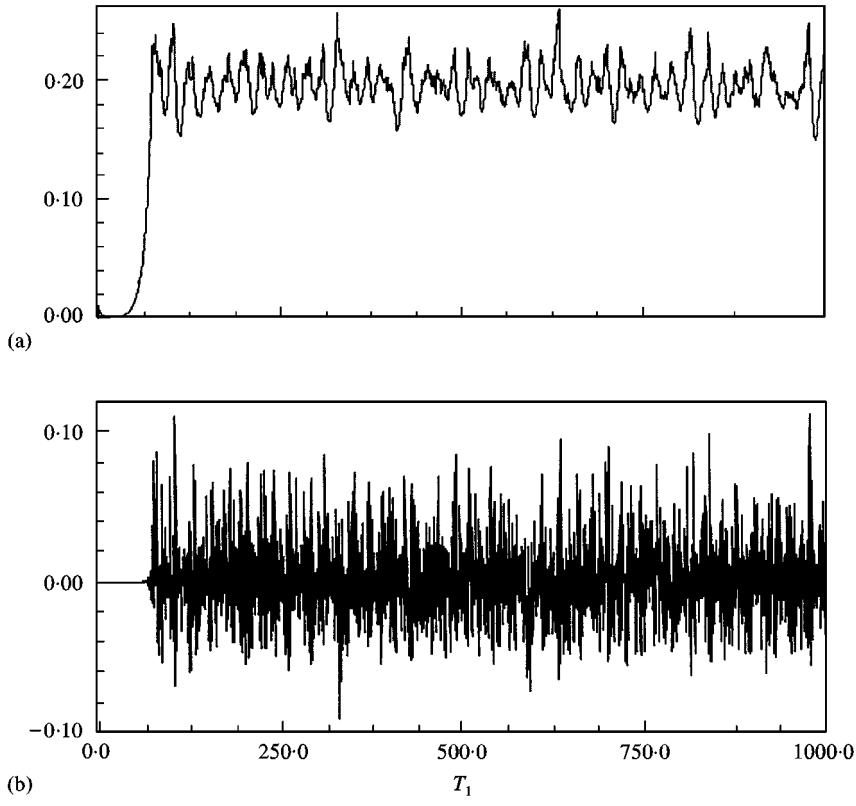

Figure 5. Time history records of response amplitudes for the impact case under first-mode parametric excitation for $Y_0 = 0{\cdot}2$, $\mu = 0{\cdot}2$, $\lambda = 0{\cdot}2$, $\sigma_y = 0{\cdot}0$, $\sigma_I = 0{\cdot}0$, $\zeta_1 = \zeta_2 = 0{\cdot}1$, $C_{16} = -0{\cdot}05$, $C_{15} = -0{\cdot}05$, and initial conditions (a) $(T_1 = 0) = 0{\cdot}01$, (*b*) $(T_1 = 0) = 0{\cdot}01$.

$$\omega_1 = -\omega_1^2\bar{\zeta}_1 a + \left(\frac{G_{118}\omega_2}{8}\cos\gamma_2 - \bar{G}_6\sin\gamma_2\right)a^2 b + \frac{\omega_1}{16}C_{15}a^5$$

$$-\frac{3\omega_1}{8}C_{15}a^4 b\cos\gamma_2 + \frac{3\omega_1}{8}C_{15}a^3 b^2 - \left(\bar{G}_7\cos\gamma_2 - \frac{15\omega_2}{16}C_{15}^3\sin\gamma_2\right)a^2 b^3$$

$$+\bar{G}_3 a b^4, \tag{28}$$

$$\frac{\partial\gamma_2}{\partial T_1} = \sigma_I + \frac{G_{22}}{4\omega_2}Y_0\sin\gamma_1 - \left(3\frac{\bar{G}_2}{\omega_1} - \frac{\bar{G}_8}{\omega_2}\right)a^2 - \left(3\frac{\bar{G}_1}{\omega_1} - \frac{\bar{G}_9}{\omega_2}\right)b^2$$

$$-\frac{3}{\omega_1}\left(\frac{G_{118}\omega_2}{8}\sin\gamma_2 + \bar{G}_6\cos\gamma_2\right)ab + \frac{\bar{G}_{11}}{\omega_2}\frac{a^3}{b}\cos\gamma_2$$

$$+\frac{5}{16}C_{16}\left(\frac{1}{\omega_1} - \frac{1}{\omega_2}\right)a^4 + \left(\frac{9}{8}C_{15} + \frac{\bar{G}_{12}}{\omega_2}\right)a^3 b\sin\gamma_2$$

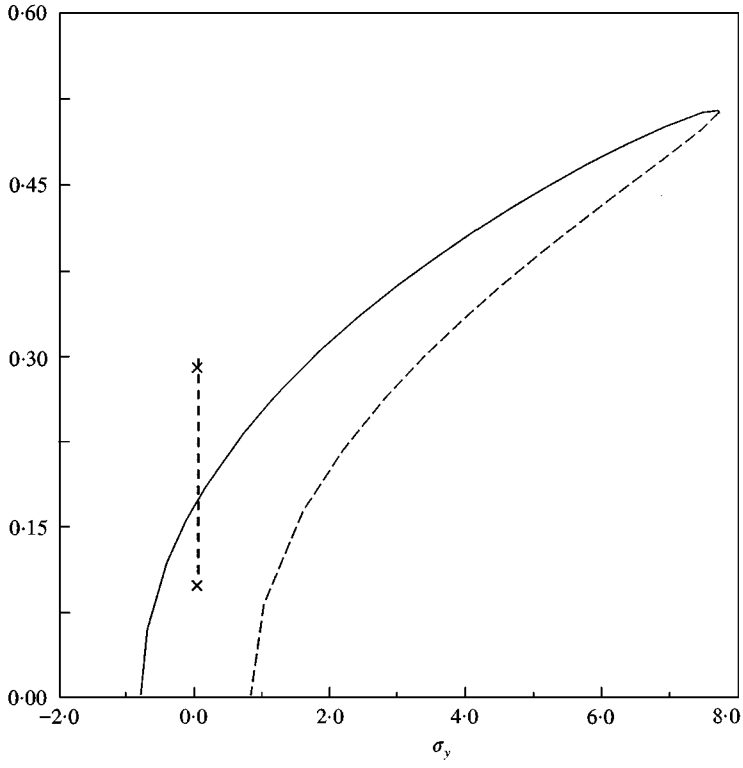

Figure 6. First-mode amplitude–frequency response curve in the absence of internal resonance [16] showing the response amplitude (dotted vertical line between two crosses) at $\sigma_y = 0{\cdot}0$ when the system is internally tuned for $\sigma_I = 0{\cdot}0$, $Y_0 = 0{\cdot}2$, $\mu = 0{\cdot}2$, $\lambda = 0{\cdot}2$, $\zeta_1 = \zeta_2 = 0{\cdot}1$.

$$+\left(3\frac{\bar{G}_4}{\omega_1}+\frac{\bar{G}_{10}}{\omega_2}\right)a^2b^2+\frac{3}{\omega_1}\left(\bar{G}_7\sin\gamma_2-\frac{15}{16}C_{15}\omega_2\cos\gamma_2\right)ab^3$$

$$-\frac{5}{8}C_{16}\left(\frac{9}{\omega_1}-\frac{1}{2\omega_2}\right)b^4+\frac{1}{32}(\omega_1C_{15}\sin\gamma_2+5C_{16}\cos\gamma_2)\frac{a^5}{b}, \tag{29}$$

$$\omega_2\frac{\partial b}{\partial T_1}=-\frac{1}{4}G_{22}bY_0\cos\gamma_1-\omega_2^2\bar{\zeta}_2b-\bar{G}_{11}a^3\sin\gamma_2+\frac{1}{32}C_{15}(\omega_1\cos\gamma_2-5C_{15}\sin\gamma_2)a^5$$

$$+\frac{3\omega_1}{16}C_{15}a^4b+\bar{G}_{12}a^3b^2\cos\gamma_2+\frac{\omega_2}{16}C_{15}b^5. \tag{30}$$

Equations (27)–(30) define the response amplitudes and phase angles in the neighborhood of the simultaneous parametric resonance condition $\Omega_y = 2\omega_2$ and internal resonance condition $\omega_2 = 3\omega_1$. The response can be obtained by setting the left-hand side to zero.

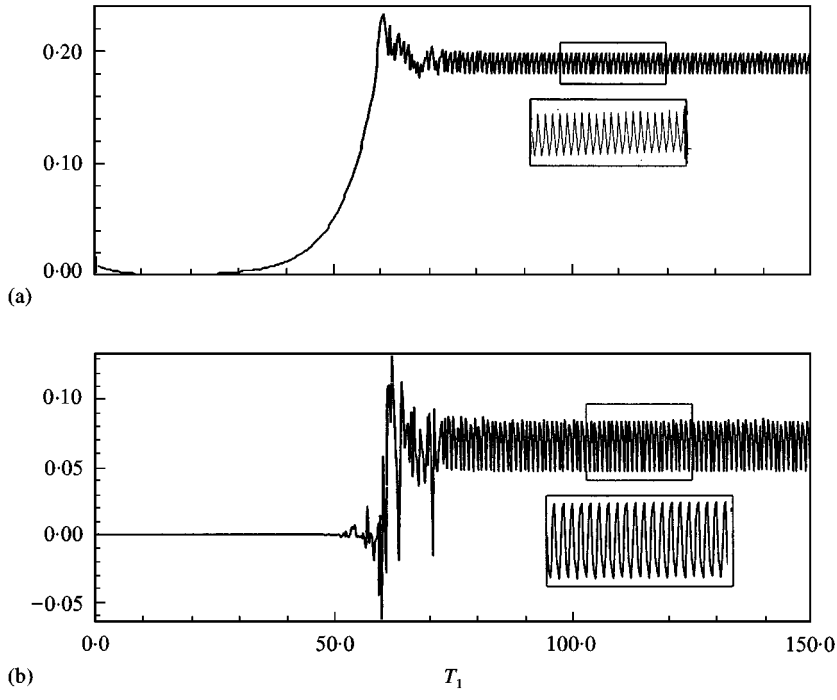

Figure 7. Quasi-periodic time history records of response amplitudes for the impact case under first-mode parametric excitation for $Y_0 = 0{\cdot}2$, $\mu = 0{\cdot}2$, $\lambda = 0{\cdot}2$, $\sigma_y = 0{\cdot}0$, $\sigma_I = -10$, $\zeta_1 = \zeta_2 = 0{\cdot}1$, $C_{16} = -0{\cdot}05$, $C_{15} = -0{\cdot}05$, and initial conditions (a) $(T_1 = 0) = 0{\cdot}01$, (b) $(T_1 = 0) = 0{\cdot}01$.

The non-impact response is examined by dropping the quintic terms from equations (27)–(30). The amplitude and phase equations take the form

$$\frac{\partial \gamma_1}{\partial T_1} = \sigma_y + \frac{2}{\omega_2}\left\{G_{22}\frac{Y_0}{4}\sin\gamma_1 + \bar{G}_6 a^2 + \bar{G}_8 a^2 + \bar{G}_9 b^2 + \bar{G}_{11}\frac{a^3}{b}\cos\gamma_2\right\}, \quad (31)$$

$$\omega_1 \frac{\partial a}{\partial T_1} = -\omega_1^2 \bar{\zeta}_1 a + \frac{G_{118}\omega_2}{8} a^2 b \cos\gamma_2 - \bar{G}_6 a^2 b \sin\gamma_2, \quad (32)$$

$$\frac{\partial \gamma_2}{\partial T_1} = \sigma_I + \frac{G_{22}}{4\omega_2} Y_0 \sin\gamma_1 - \left(3\frac{\bar{G}_2}{\omega_1} - \frac{\bar{G}_8}{\omega_2}\right)a^2 - 3\left(\frac{\bar{G}_1}{\omega_1} - \frac{\bar{G}_9}{\omega_2}\right)b^2 - \frac{3}{\omega_1}\left(\frac{G_{118}\omega_2}{8}\sin\gamma_2 + \bar{G}_6\cos\gamma_2\right)ab + \frac{\bar{G}_{11}}{\omega_2}\cos(\gamma_2)\frac{a^3}{b}, \quad (33)$$

$$\omega_2 \frac{\partial b}{\partial T_1} = -G_{22} b \frac{Y_0}{4}\cos\gamma_1 - \omega_2^2 \bar{\zeta}_2 b - \bar{G}_{11} a^3 \sin\gamma_2. \quad (34)$$

Careful inspection of these equations for the steady state solution reveals that the resulting three algebraic equations [from equations (31), (33) and (34)] are in two unknowns, namely b and γ_1. This means that the time derivative of γ_2 may not vanish. Note that if the left-hand sides are set to zero one may get more than one solution. These solutions include the unimodal response which can be obtained in

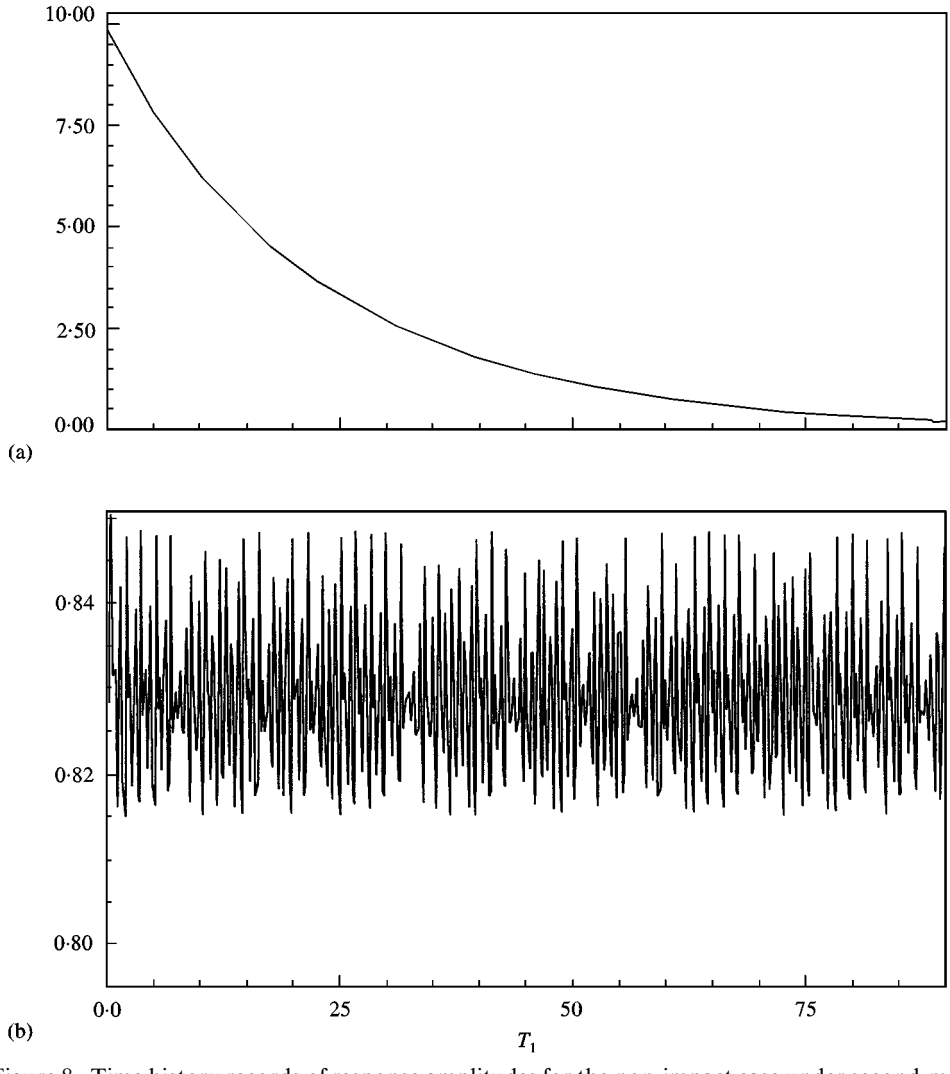

Figure 8. Time history records of response amplitudes for the non-impact case under second-mode parametric excitation for $Y_0 = 0{\cdot}2$, $\mu = 0{\cdot}2$, $\lambda = 0{\cdot}2$, $\sigma_y = -50$, $\sigma_I = 0{\cdot}0$, $\zeta_1 = \zeta_2 = 0{\cdot}1$, and initial conditions (a) $(T_1 = 0) = 0{\cdot}1$, (b) $(T_1 = 0) = 0{\cdot}086$.

the absence of internal resonance (see reference [16]):

$$a = 0, \quad b = 0 \text{ or } \quad b_{1,2}^2 = \frac{1}{4\bar{G}_9}\{2\omega_2\sigma_y \pm \sqrt{\bar{G}_{22}^2 Y_0^2 - 16\omega_2^4 \bar{\zeta}_2^2}\}. \tag{35}$$

The validity of these solutions is examined by integrating equations (31)–(34) numerically for mass ratio $\mu = 0{\cdot}2$, length ratio $\lambda = 0{\cdot}2$, local frequency ratio $v = 0{\cdot}5$, excitation amplitude ratio $Y_0 = 0{\cdot}1$ and damping ratio $\zeta_1 = \zeta_2 = 0{\cdot}1$. Figures 8 show that the first modal amplitude always reaches its zero equilibrium, while the second modal amplitude may or may not reach a fixed value depending on the initial conditions. When the second mode does not reach steady state value,

the first phase angle always varies with time, while the second phase angle has a constant time rate. For different set of initial conditions, the second-mode amplitude reaches a fixed point; however, its phase has a constant time rate, while the second phase possesses fixed steady state values.

The numerical integration always yields a unimodal response regardless of the the value of the internal detuning parameter and initial conditions and no energy transfer from the second mode to the first one. For zero internal detuning parameter $\sigma_I = 0$, the unimodal response is always a fixed point but takes two different values depending on the initial conditions over a parametric detuning parameter σ_y ranging from 0 to (-40). For $\sigma_y < -40$, the response exhibits two possible different solutions; one is fixed while the other is chaotic. For the chaotic response, equations (31)–(34) do not achieve a steady state for relatively large initial conditions while they achieve a fixed point for smaller initial conditions. It is also found that the internal detuning parameter does not have any appreciable effect on the response except when the internal detuning parameter assumes very large values. The initial conditions can bring the response either to a fixed point or to periodic/quasi-periodic oscillations.

Figure 9 summarizes the different scenarios described earlier. It shows the amplitude–frequency response curves in the absence of internal resonance as

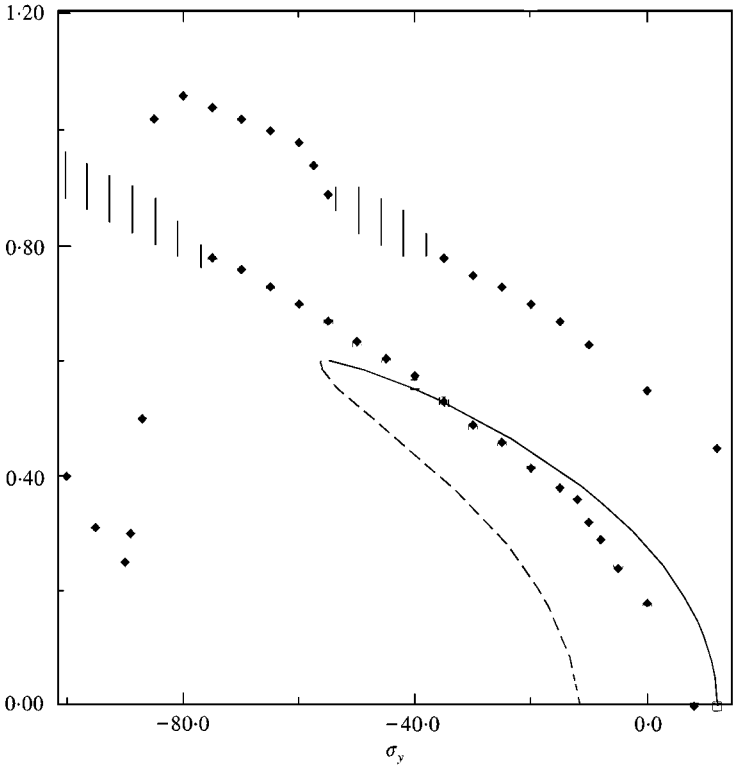

Figure 9. Second-mode amplitude–frequency response for the non-impact case showing the response in the absence of internal resonance (solid and dashed curves taken from reference [16]) and in the presence of internal resonance (◆) and vertical lines for $\sigma_I = 0{\cdot}0$.

indicated by the solid and dashed curves (taken from reference [16]). The solid diamond points belong to the response with zero internal detuning parameter. Over the larger portion of the parametric detuning parameter there are two different manifolds indicated by two solid diamonds for each value of σ_y up to $\sigma_y = -40$. There is a region showing one solid diamond (indicating fixed solution) and a vertical short line indicating chaotic behavior.

In the presence of impact, equations (27)–(30) are considered. For the steady state solution, the left-hand sides are set to zero. The resulting algebraic equations are three in two unknowns which implies that a steady state response is not possible at least for the second phase angle. Thus, equations (27)–(30) are numerically integrated for mass ratio $\mu = 0{\cdot}2$, length ratio $\lambda = 0{\cdot}2$, local frequency ratio $\nu = 0{\cdot}5$, excitation amplitude ratio $Y_0 = 0{\cdot}1$, $C_{16} = -0{\cdot}5$, $C_{15} = -0{\cdot}05$ and damping ratio $\zeta_1 = \zeta_2 = 0{\cdot}1$. The first-mode amplitude always reaches its zero equilibrium position while the second-mode amplitude reaches fixed solutions depending on the initial conditions. However, the first phase angle reaches a non-zero fixed value while the second phase angle increases linearly with time. This means that $\mathrm{d}\gamma_2/\mathrm{d}T_1 \neq 0$ and any analytical solution is not valid.

For zero internal detuning parameter σ_I and different values of parametric detuning parameter σ_y, the response amplitude always reaches a fixed steady state value. For each parametric detuning parameter there are two different values of the second-mode amplitude corresponding to two different sets of initial conditions. It is important to note that the amplitude b reaches two different values for the same parametric detuning parameter and for zero internal detuning parameter. In the absence of internal resonance approaches the value determined solely by second-mode parametric excitation.

Figure 10 shows the amplitude frequency response curves as estimated by second-mode excitation in the absence of internal resonance (taken from reference [16]). The solid curves belong to stable manifolds while the dotted ones are unstable. In the presence of internal resonance $\sigma_I = 0$, the response is indicated by two solid diamonds which are increasing with the negative values of the parametric detuning parameter up to one of the tuning points $\sigma_y \approx -50$. For values $\sigma_y < -50$, the trend is changed. For very large values of $\sigma_I = 0$, the response indicated by empty squares is very close to the solid curve (of second parametric excitation). The agreement holds for a range of parametric detuning parameter defined by the region $\sigma_y = 0$ to -30. For $\sigma_y < -30$, there is a deviation attributed to the effect of the time variation of phase angles.

Introducing the detuning parameters σ_y and σ_I defined by $\Omega_y = \omega_1 + \omega_2 + \varepsilon\sigma_y$, $\omega_2 = 3\omega_1 - \varepsilon\sigma_I$, and following the standard procedure of multiple scales gives the following set of first-order differential equations in the amplitudes a and b and phases angles $\gamma_1 = \sigma_y T_1 - \alpha - \beta$, $\gamma_2 = \sigma_I T_1 - \beta + 3\alpha$:

$$\frac{\partial\gamma_1}{\partial T_1} = \sigma_y + \frac{Y_0}{4}\left(\frac{G_{12}}{\omega_1}\frac{b}{a} + \frac{G_{22}}{4}\frac{a}{b}\right)\sin\gamma_1 + \left(\frac{\bar{G}_1}{\omega_1} - \frac{\bar{G}_9}{\omega_2}\right)b^2 + \left(\frac{\bar{G}_2}{\omega_1} + \frac{\bar{G}_6 + \bar{G}_8}{\omega_2}\right)a^2$$

$$+ \frac{1}{\omega_1}\left(\frac{G_{118}\omega_2}{8}\sin\gamma_2 + \bar{G}_6\cos\gamma_2\right)ab + \frac{\bar{G}_{11}}{\omega_2}\frac{a^3}{b}\cos\gamma_2$$

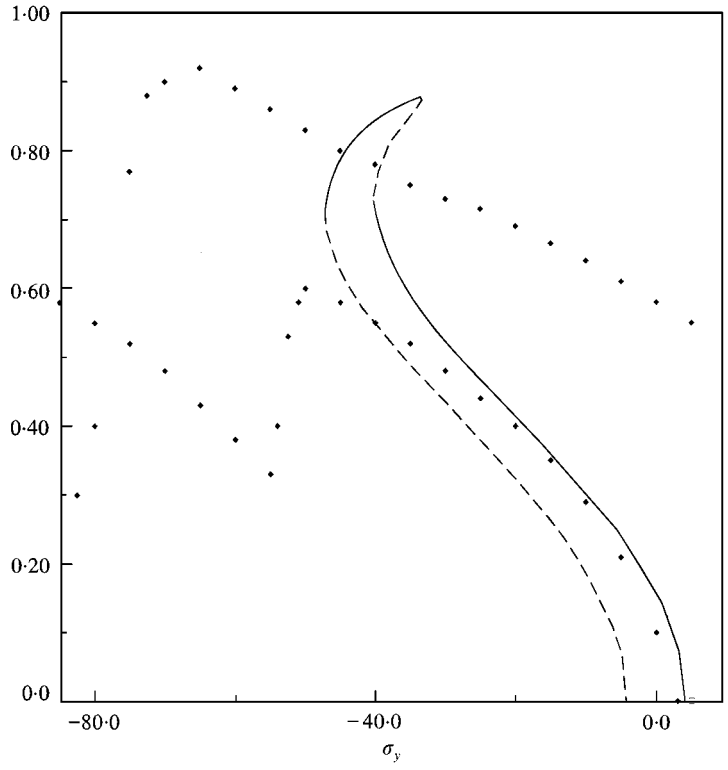

Figure 10. Second-mode amplitude–frequency response for the impact case showing the response in the absence of internal resonance (solid and dashed curves taken from reference [16]) and in the presence of internal resonance (◆) for $\sigma_I = 0{\cdot}0$.

$$-\left(\frac{\bar{G}_4}{\omega_1}-\frac{\bar{G}_{10}}{\omega_2}\right)a^2b^2+\frac{5}{16}C_{16}\left(\frac{6}{\omega_1}+\frac{1}{\omega_2}\right)b^4+\frac{5}{16}C_{16}\left(\frac{1}{\omega_1}+\frac{3}{\omega_2}\right)a^4$$

$$-\left(\frac{3}{8}C_{15}-\frac{G_{12}}{\omega_2}\right)a^3b\sin\gamma_2-\frac{1}{\omega_1}\left(\bar{G}_7\sin\gamma_2-\frac{15}{16}C_{15}\omega_2\cos\gamma_2\right)ab^3$$

$$+\frac{1}{32\omega_2}\frac{a^5}{b}(\omega_1C_{15}\sin\gamma_2+5C_{16}\cos\gamma_2), \tag{36}$$

$$\omega_1\frac{\partial a}{\partial T_1}=-G_{12}b\frac{Y_0}{4}\cos\gamma_1-\omega_1^2\bar{\zeta}_1a+\frac{G_{118}\omega_2}{8}a^2b\cos\gamma_2-\bar{G}_6a^2b\sin\gamma_2+\frac{\omega_1}{16}C_{15}a^5$$

$$-\frac{3\omega_1}{8}C_{15}a^4b\cos\gamma_2+\frac{3\omega_1}{8}C_{15}a^3b^2$$

$$-\left(\bar{G}_7\cos\gamma_2+\frac{15\omega_2}{16}C_{15}\sin\gamma_2\right)a^2b^3+\bar{G}_3ab^4, \tag{37}$$

$$\frac{\partial \gamma_2}{\partial T_1} = \sigma_I + \frac{1}{4}\left(\frac{3}{\omega_1} G_{12}\frac{b}{a} - \frac{G_{23}}{\omega_2}\frac{a}{b}\right) Y_0 \sin\gamma_1 - \left(3\frac{\bar{G}_2}{\omega_1} - \frac{\bar{G}_8}{\omega_2}\right)a^2 - \left(3\frac{\bar{G}_1}{\omega_1} - \frac{\bar{G}_9}{\omega_2}\right)b^2$$
$$- \frac{3}{\omega_1}\left(\frac{G_{118}\omega_2}{8}\sin\gamma_2 + \bar{G}_6\cos\gamma_2\right)ab + \frac{\bar{G}_{11}}{\omega_2}\cos\gamma_2\left(\frac{a^3}{b}\right)$$
$$- \frac{15}{16}C_{16}\left(\frac{1}{\omega_1} - \frac{1}{\omega_2}\right)a^4 + \left(\frac{3}{8}C_{15} + \frac{\bar{G}_{12}}{\omega_2}\right)a^3 b\sin\gamma_2 + \left(3\frac{\bar{G}_4}{\omega_1} + \frac{\bar{G}_{10}}{\omega_2}\right)a^2b^2$$
$$+ \frac{3}{\omega_1}\left(\bar{G}_7\sin\gamma_2 - \frac{15}{16}C_{15}\omega_2\cos\gamma_2\right)ab^3 - \frac{5}{8}C_{16}\left(\frac{9}{\omega_1} - \frac{1}{2\omega_2}\right)b^4$$
$$+ \frac{1}{32\omega_2}(\omega_1 C_{15}\sin\gamma_2 + 5C_{16}\cos\gamma_2)\frac{a^5}{b}, \tag{38}$$

$$\omega_2\frac{\partial b}{\partial T_1} = -G_{23}a\frac{Y_0}{4}\cos\gamma_1 - \omega_2^2\bar{\zeta}_2 b - \bar{G}_{11}a^3\sin\gamma_2 + \frac{3\omega_1}{16}C_{15}a^4 b + \frac{\omega_2}{16}C_{15}b^5$$
$$+ \bar{G}_{12}a^3b^3\cos\gamma_2 + \frac{C_{15}}{32}(\omega_1\cos\gamma_2 - 5\sin\gamma_2)a^5. \tag{39}$$

These equations are integrated numerically for mass ratio $\mu = 0{\cdot}2$, length ratio $\lambda = 0{\cdot}2$, local frequency ratio $\nu = 0{\cdot}5$, excitation amplitude ratio $Y_0 = 0{\cdot}1$, and damping ratios $\zeta_1 = \zeta_2 = 0{\cdot}1$.

First we consider the non-impact response which is examined by dropping the quintic terms from equations (36)–(39). For the steady state solution, the left-hand sides of the resulting equation are set to zero. Careful inspection of the algebraic equations reveals the possibility of two equilibrium positions which can only take place when the phase angles take the two specific values $\gamma_1 = \gamma_2 = 0$ or π. The corresponding steady state solutions are

$$a = -\frac{4\omega_2^2\bar{\zeta}_2}{G_{23}Y_0}b \tag{40}$$

and from equation (20) one obtains

$$b = 0 \text{ or } b = \pm\frac{1}{2\omega_2^2\bar{\zeta}_2}\sqrt{\frac{|G_{12}G_{23}Y_0^2 - 4\omega_1^2\omega_2^2\bar{\zeta}_1\bar{\zeta}_2|G_{23}Y_0}}{2G_{118}}}. \tag{41a, b}$$

Another solution is given by equation (23) and

$$b = \pm\sqrt{\left(\sigma_y + \frac{\sigma_I}{3}\right)\Big/\left[\frac{4\bar{G}_9}{3\omega_2} - \frac{16\omega_2^4\bar{\zeta}_2^2}{\bar{G}_{23}^2Y_0^2}\left(\frac{1}{\omega_2}\left(\bar{G}_6 + \frac{\bar{G}_8}{3}\right) - \frac{16\omega_2\bar{G}_{11}\bar{\zeta}_2}{3\bar{G}_{23}Y_0}\right)\right]}, \tag{42}$$

Note that the zero solution, given in equation (41a), corresponds to the static equilibrium position, while the other two solutions (41b) and (42) can only exist under parametric excitation, i.e. when $Y_0 \neq 0$. Obviously, the solution spirals out about each of the two unstable equilibrium points given by equations (41b) or (42) until its amplitude is sufficiently large when it is attracted to the other equilibrium

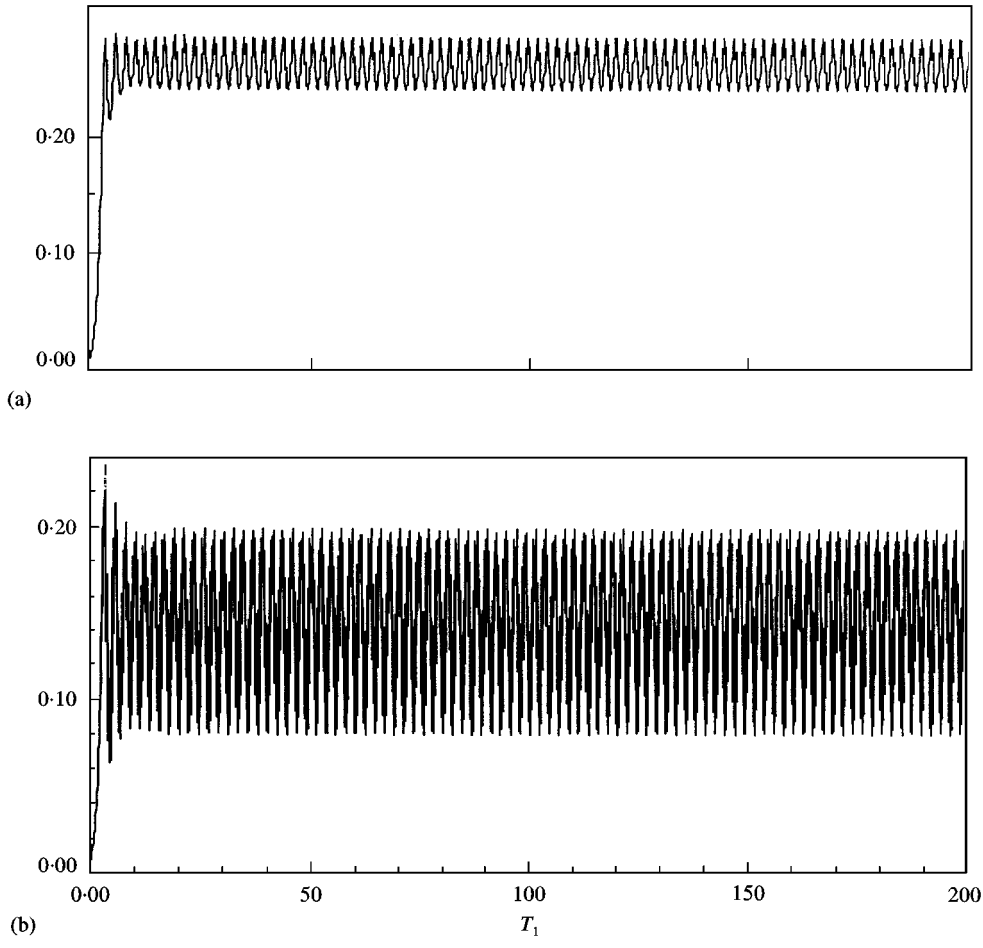

Figure 11. Time history records of response amplitudes for the non-impact case under mixed-mode parametric excitation for $Y_0 = 0{\cdot}2$, $\mu = 0{\cdot}2$, $\lambda = 0{\cdot}2$, $\sigma_y = 0$, $\sigma_I = -30$, $\zeta_1 = \zeta_2 = 0{\cdot}1$, and initial conditions (a) $(T_1 = 0) = 0{\cdot}1$, (b) $(T_1 = 0) = 0{\cdot}086$.

point about which it then spirals. The jumping of the solution trajectory from the vicinity of one unstable equilibrium point to the other unstable point seems to take place in a random fashion. The alternation of the second mode between two states reflects the chaotic nature of the system similar to the case of the Lorenz attractor [19].

If $\gamma_1 \neq \gamma_2 \neq 0$, it is not possible to solve for the stationary response. In this case, the equations of motion are numerically integrated. Depending on the internal detuning parameter and initial conditions, the numerical integration gives different response regimes. For zero detuning parameters, the response amplitudes of the two modes experience quasi-periodic oscillations. If one changes the initial conditions the response trajectories take another form of attractor of nearly periodic oscillations. In the absence of internal resonance, the amplitude frequency curves give fixed points corresponding to steady state responses under purely

parametric excitation. The presence of internal resonance obviously results in quasi-periodic motion and the energy is re-distributed between the two modes.

For an internal detuning parameter, $\sigma_I = -30$, and exact parametric resonance, the response can be quasi-periodic as shown in Figure 11(a) or chaotic with irregular jumps between two unstable equilibria as shown in Figure 12(a) depending on initial conditions. Figure 11(b) shows the phase of the first mode is periodic while it has constant time rate for the second mode. On the other hand, the phase of the switching sign of the amplitude b shown in Figure 12(b) reveals that the phase of the first mode assumes fixed values when the amplitude fluctuates around the positive value. When the first mode amplitude fluctuates around the negative value the corresponding phase increases monotonically with time. The spectra of Figure 12(a) reveal that the second mode amplitude has a wide frequency spectrum with a large number of closely packed peaks which fall off rapidly as their frequency increases. The response is sensitive to initial conditions and different initial

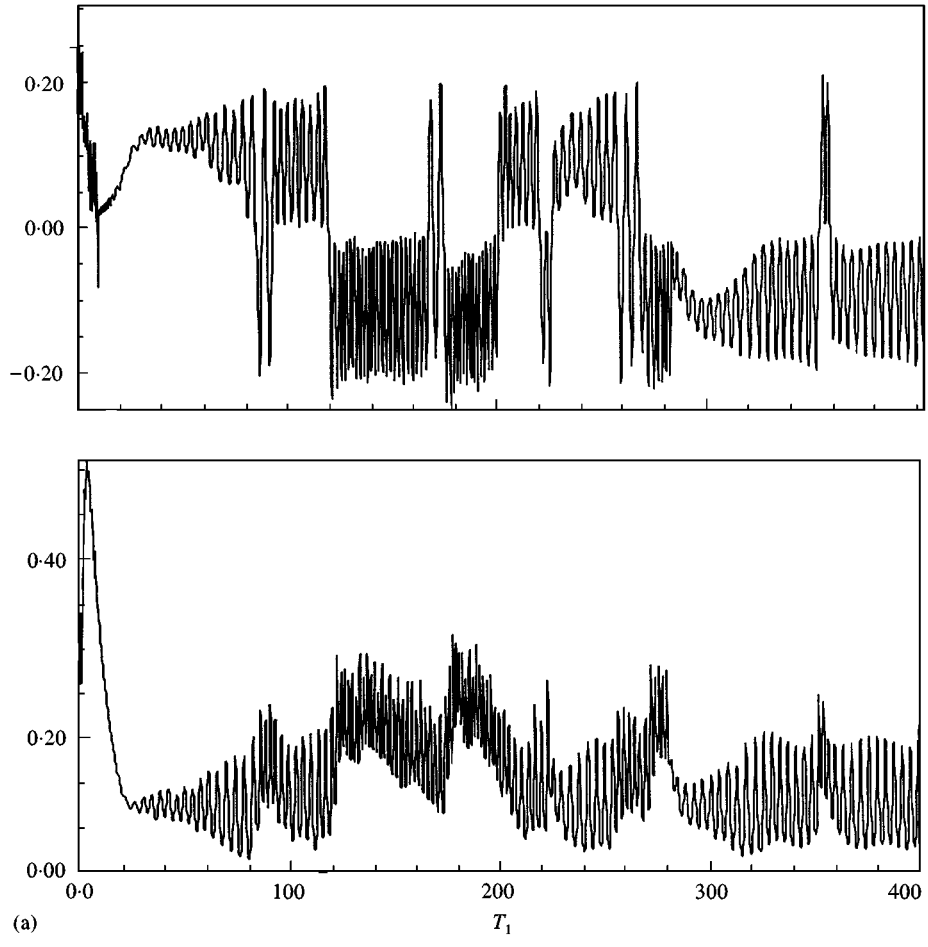

Figure 12. (a) Time history records of response amplitudes for the non-impact case under mixed mode parametric excitation; (b) time history records of response phases for $Y_0 = 0{\cdot}2$, $\mu = 0{\cdot}2$, $\lambda = 0{\cdot}2$, $\sigma_y = 0$, $\sigma_I = -30$, $\zeta_1 = \zeta_2 = 0{\cdot}1$, and initial conditions (1) $(T_1 = 0) = 0{\cdot}2$, (2) $(T_1 = 0) = 0{\cdot}2$.

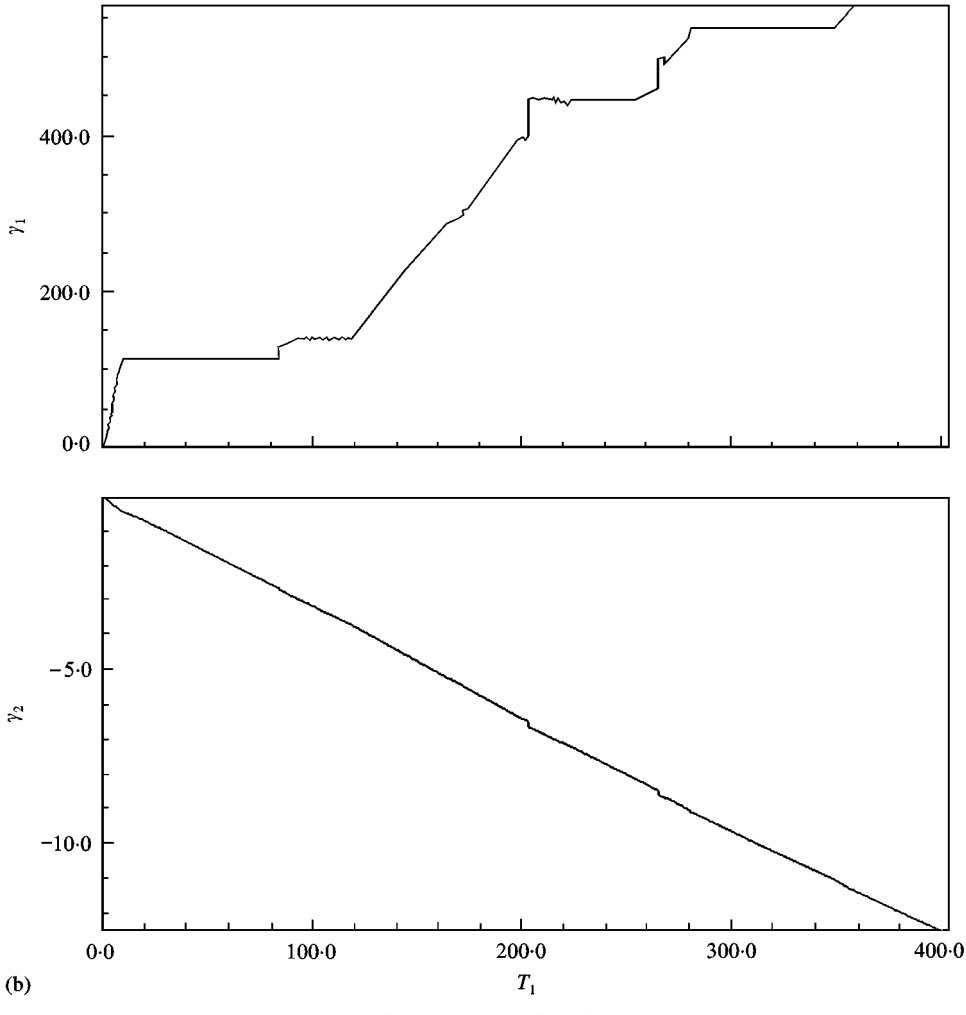

Figure 12. Continued.

conditions can lead to almost periodic response. The initial conditions have a significant effect on the response behavior.

Contrary to the non-impact case, the impact loading brings the system response to a fixed stationary point at exactly zero detuning parameters $\sigma_I = 0$, and $\sigma_Y = 0$. The presence of internal resonance results in a redistribution of energy between the two modes. Over a very narrow internal detuning parameter, $0 < \sigma_I < 1$, the system preserves fixed-point response. Away from this region, the response is essentially quasi-periodic over the two ranges of internal detuning parameter $-15 < \sigma_I < 0$, and $1 < \sigma_I < 15$. The response for these ranges of internal detuning possesses different attractors with different periods. Beyond these ranges, the response experiences complex characteristics where both quasi-periodic and switching phase characteristics can take place depending on the initial conditions. Figures 13(a) and 13(b) show two sets of time history records corresponding to

different sets of initial conditions and for the same internal detuning parameter $\sigma_I = -15$. This trend continues for different values of σ_I. An extensive number of numerical integration has revealed the presence of three possible basic regimes: fixed point, quasi-periodic, and quasi-periodic/switching phase regimes. Again each regime is governed by the initial conditions, internal detuning parameter, damping ratios and excitation amplitude.

4. CONCLUSIONS

The dynamic response of a non-linear-coupled oscillator, involving impact forces, to parametric excitation in the presence of simultaneous occurrence of parametric and internal resonance conditions is examined. The method of multiple scales has been used to derive four first-order differential equations for the response amplitudes and phases in the absence and in the presence of impact forces. When

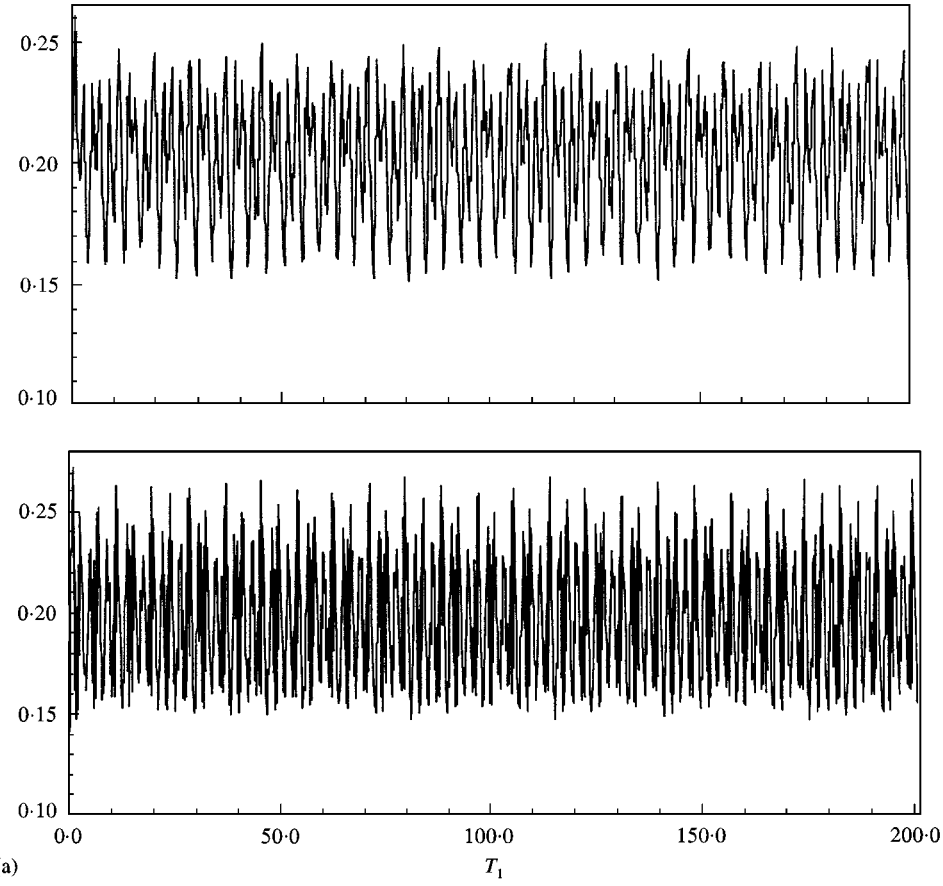

Figure 13. (a) Time history records of response amplitudes for the impact case under mixed mode parametric excitation for initial conditions (1) $(T_1 = 0) = 0{\cdot}2$, (2) $(T_1 = 0) = 0{\cdot}2$; (b) for initial conditions (1) $(T_1 = 0) = 0{\cdot}01$, (2) $(T_1 = 0) = 0{\cdot}01$. Both figures are obtained for $C_{16} = -0{\cdot}05$, $C_{15} = -0{\cdot}05$, $Y_0 = 0{\cdot}2$, $\mu = 0{\cdot}2$, $\lambda = 0{\cdot}2$, $\sigma_y = 0$, $\sigma_I = -15$, $\zeta_1 = \zeta_2 = 0{\cdot}1$.

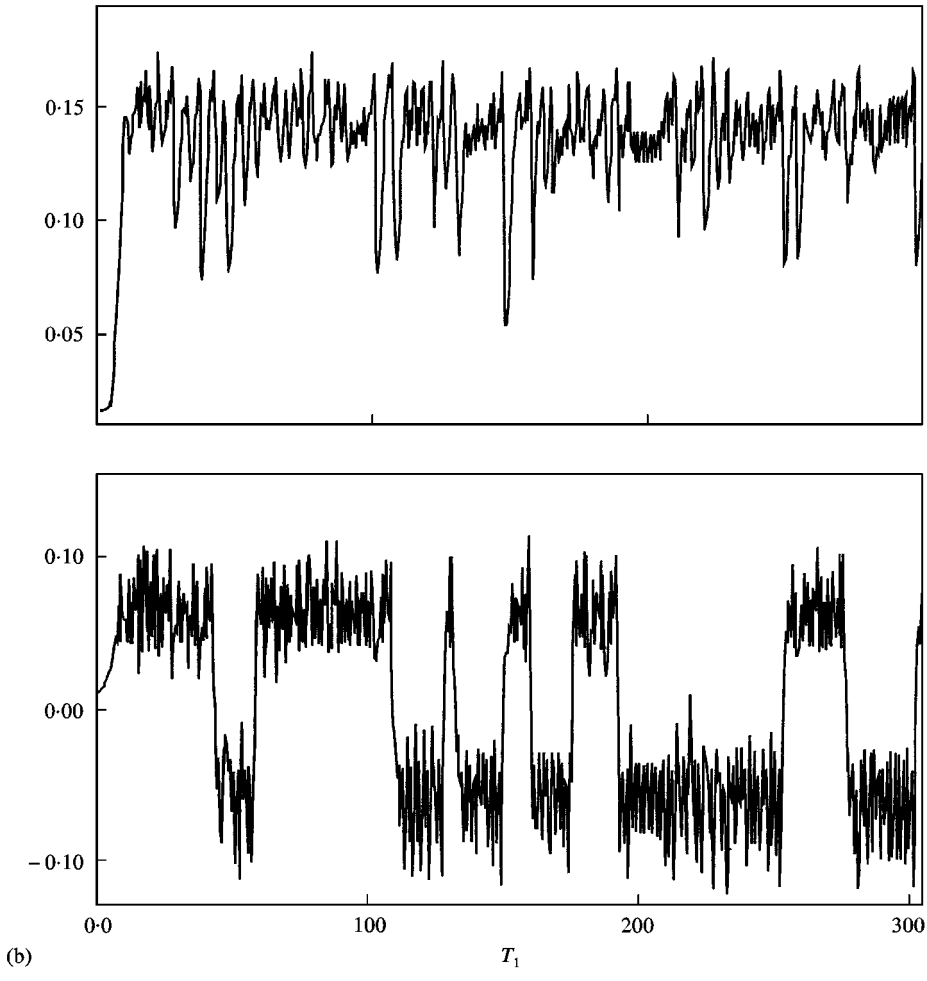

Figure 13. Continued.

the first mode is parametrically excited, the numerical integration yielded fixed or non-stationary solutions depending on initial conditions for non-impact and impact cases. In the absence of impact forces, the second mode, which is indirectly excited experiences wide spectrum response with random behavior looking. Fixed solution were obtained for internal detuning parameter well remote from exact internal resonance. The system response is found to possess two basins of initial conditions. One set of initial conditions can lead the system response to oscillate about the fixed point of the unimodal response ($a \neq 0$ and $b = 0$) in the absence of internal resonance. The other set can drag the response to chaotic motion about non-zero mean values of both modes. There are occasional symmetric spikes indicating that these response possesses are essentially non-Gaussian with zero skewness and kurtosis greater than 3. In the presence of impact forces, the scenario was changed and the response of the second mode becomes random with almost asymmetric non-Gaussian distribution.

Under second-mode parametric excitation, it is found that the system energy is more localized in the second mode with no energy sharing with the first mode. While fixed amplitude solutions were obtained, the corresponding phase angles were changing with time. In the absence of impact, the response exhibits fixed and chaotic solutions depending on initial conditions. In the presence of impact the second-mode amplitude always reaches steady state. In all cases, the response did not coincide with the response of second-mode excitation (in the absence of internal resonance) mainly due to time variation of the phase angles.

Under mixed-mode parametric excitation, and in the absence of impact loading, the response did not achieve any stationary state regardless of initial conditions and internal detuning parameter. The chaotic motion experienced oscillations around two unstable equilibria indicating phase switching. Under restricted conditions of zero-phase angles, fixed solutions are obtained. In the presence of impact loading, the system possesses only fixed point within a very narrow range of internal detuning parameter. Away from this region, the response is found to be quasi-periodic or chaotic depending on initial conditions and internal detuning parameter. It is important to note that other factors such as damping ratios and excitation amplitudes can play an important role in shaping the response characteristics.

ACKNOWLEDGMENT

This research is supported by National Science Foundation grant no. CMS-9634223, and by the Institute for Manufacturing Research at Wayne State University. The second author would like to thank the Egyptian Channel Program for the financial support during his studies at Wayne State University. Both authors would like to thank Professor Valery N. Pilipchuk for the fruitful discussion on the results of this research.

REFERENCES

1. A. L. Kunitsyn 1971 *Journal of Applied Mathematics and Mechanics* (*PMM*) **35**, 164–167. On the stability of pure imaginary roots in the critical case in the presence of intrinsic resonance.
2. G. G. Khazina 1974 *Journal of Applied Mathematics and Mechanics* (*PMM*) **38**, 43–51. Certain stability in the presence of resonances.
3. Ia. M. Goltser and A. L. Kuntisyn 1975 *Journal of Applied Mathematics and Mechanics* (*PMM*) **39**, 974–984. On the stability of autonomous systems with intrinsic resonance.
4. A. L. Kunitsyn and M. V. Matveyev 1991 *Journal of Applied Mathematics and Mechanics* (*PMM*) **55**, 780–788. The stability of a class of reversible systems.
5. E. V. Aa and J. A. Sanders 1979 *Asymptotic Analysis from Theory to Application* (F. Verhulst, editor), Lecture Notes in Mathematics, Vol. 711, 187–208. Berlin: Springer-Verlag. The 1 : 2 : 1-resonance, its periodic orbits and integrals.
6. A. L. Kunitsyn and A. P. Markeev 1979 *Achievements of Science and Technology, General Mechanics*, Vol. 4. Moscow: Viniti: Stability in resonance cases.
7. A. L. Kunitsyn and A. A. Perezhogin 1985 *Journal of Applied Mathematics and Mechanics* (*PMM*) **49**, 53–57. The stability of neutral systems in the case of a multiple fourth-order resonance.

8. A. L. KUNITSYN and A. A. TUYAKBAYEV 1992 *Journal of Applied Mathematics and Mechanics* (*PMM*) **56**, 572–576. The stability of Hamiltonian systems in the case of a multiple fourth-order resonance.
9. A. L. KUNITSYN and A. S. MURATOV 1993 *Journal of Applied Mathematics and Mechanics* (*PMM*) **57**, 247–255. The stability of a class of quasi-autonomous periodic systems with internal resonance.
10. V. F. ZHURAVLEV 1992 *Journal of Applied Mathematics and Mechanics* (*PMM*) **56**, 725–735. Oscillations shape control in resonant systems.
11. V. I. BABITSKY 1978 *Theory of Vibro-impact Systems*. Moscow: Nauka (in Russian).
12. K. H. HUNT and F. R. E. GROSSLEY 1975 *ASME Journal of Applied Mechanics* **97**, 440–445. Coefficient of restitution interpreted as damping in vibro-impact.
13. E. G. VEDENOVA, L. I. MANEVICH and V. N. PILIPCHUK 1985 *Pricladnaya Matematika Mekhanika* (*PMM*) **49**, 153–159. Normal oscillations of a string with concentrated masses on nonlinear supports.
14. J. SHAW and S. W. SHAW 1989 *ASME Journal of Applied Mechanics* **46**, 168–174. The onset of chaos in a two-degree-of-freedom impacting system.
15. V. N. PILIPCHUK and R. A. IBRAHIM 1997 *Journal of Sound and Vibration* **205**, 593–615. The dynamics of a nonlinear system simulating liquid sloshing impact in moving containers.
16. M. A. EL-SAYAD, S. HANNA and R. A. IBRAHIM 1999 *Nonlinear Dynamics* **18**, 25–50. Parametric excitation of nonlinear elastic systems involving hydrodynamic sloshing impact.
17. A. H. NAYFEH and D. T. MOOK 1979 *Nonlinear Oscillations*. New York: Wiley.
18. H. N. ABRAMSON (editor) 1966 *The Dynamic Behavior of Liquids in Moving Containers*. NASA SP 106.
19. P. G. DARZIN 1992 *Nonlinear Systems*. Cambridge: Cambridge University Press.

APPENDIX A: FUNCTIONS Ψ_{ii}

The functions Ψ_{ii} of equations (6) are

$$(\Psi_{11})_{\text{gn}} = G_{18}Y_1^3 + G_{19}Y_2^3 + G_{110}Y_2^2Y_2'' + G_{111}Y_2^2Y_1'' + G_{112}Y_2Y_1Y_2''$$
$$+ G_{113}Y_2Y_1Y_1'' + G_{114}Y_1^2Y_2'' + G_{115}Y_2Y_2'^2 + G_{116}Y_1Y_2'^2 + G_{117}Y_2Y_2'Y_1'$$
$$+ G_{118}Y_1Y_2'Y_1' + G_{119}Y_1Y_2^2 + G_{120}Y_1^2Y_2 + G_{121}Y_2Y_1'^2$$
$$+ G_{122}Y_1^2Y_1'' + G_{123}Y_1Y_1'^2, \tag{A1}$$

$$(\Psi_{11})_{\text{impact}} = C_{16}Y_1^5 + C_{16}Y_2^5 + 5C_{16}Y_2Y_1^4 + 5C_{16}Y_2Y_2^4 + 4C_{15}Y_1Y_1'Y_2^3$$
$$+ 4C_{15}Y_1Y_2'Y_2^3 + 10C_{16}Y_1^2Y_2^3 + 6C_{15}Y_1'Y_1^2Y_2^2 + 10C_{16}Y_1^3Y_2^2$$
$$+ 6C_{15}Y_2'Y_1^2Y_2^2 + 4C_{15}Y_2'Y_1^3Y_2 + 4C_{15}Y_1^3Y_2Y_1'$$
$$+ C_{15}Y_1^4Y_1' + C_{15}Y_2^4Y_1' + C_{15}Y_2^4Y_2' + C_{15}Y_1^4Y_2', \tag{A2}$$

$$(\Psi_{11})_{\text{ex}} = G_{12}f_y(t)Y_2 + G_{13}f_y(t)Y_1, \tag{A3}$$

$$(\Psi_{22})_{\text{gn}} = G_{28}Y_1^3 + G_{29}Y_2^3 + G_{210}Y_2^2Y_2'' + G_{211}Y_2^2Y_1'' + G_{212}Y_2Y_1Y_2''$$
$$+ G_{213}Y_2Y_1Y_1'' + G_{214}Y_1^2Y_2'' + G_{215}Y_2Y_2'^2 + G_{216}Y_1Y_2'^2 + G_{217}Y_2Y_2'Y_1'$$
$$+ G_{218}Y_1Y_2'Y_1' + G_{219}Y_1Y_2^2 + G_{220}Y_1^2Y_2 + G_{221}Y_2Y_1'^2$$
$$+ G_{222}Y_1^2Y_1'' + G_{223}Y_1Y_1'^2, \tag{A4}$$

$$(\Psi_{11})_{\text{impact}} = C_{16}Y_1^5 + C_{16}Y_2^5 + 5C_{16}Y_2Y_1^4 + 5C_{16}Y_2Y_2^4 + 4C_{15}Y_1Y_1'Y_2^3$$
$$+ 4C_{15}Y_1Y_2'Y_2^3 + 10C_{16}Y_1^2Y_2^3 + 6C_{15}Y_1'Y_1^2Y_2^2 + 10C_{16}Y_1^3Y_2^2$$
$$+ 6C_{15}Y_2'Y_1^2Y_2^2 + 4C_{15}Y_2'Y_1^3Y_2 + 4C_{15}Y_1'Y_1^3Y_2 + C_{15}Y_1'Y_1^4$$
$$+ C_{15}Y_1'Y_2^4 + C_{15}Y_2'Y_2^4 + C_{15}Y_2'Y_1^4, \tag{A5}$$

$$(\Psi_{22})_{\text{ex}} = G_{22}f_y(t)Y_2 + G_{23}f_y(t)Y_1, \tag{A6}$$

where

$$G_{12} = \frac{1}{g}\left(1 - \frac{K_1^2}{\mu\lambda}\right), \quad G_{13} = \frac{1}{g}\left(1 + \frac{K_1K_2}{\mu\lambda}\right), \quad G_{18} = \frac{\theta_0^2}{6}\left(1 - \frac{K_1^4}{\mu\lambda^2}\right),$$

$$G_{111} = \frac{\theta_0^2K_1}{\lambda}(1+K_2)^2, \quad G_{19} = \frac{\theta_0^2}{6}\left(1 - \frac{K_1K_2^3}{\mu\lambda}\right), \quad G_{110} = \frac{\theta_0^2}{2\lambda}(K_1+K_2)(1+K_2)^2,$$

$$G_{112} = \frac{\theta_0^2}{\lambda}(K_1+K_2)(1+K_2+K_1+K_1K_2), \quad G_{113} = \frac{2\theta_0^2K_1}{\lambda}(1+K_2+K_1+K_1K_2),$$

$$G_{114} = \frac{\theta_0^2}{2\lambda}(K_1+K_2)(1+K_1)^2, \quad G_{115} = \frac{\theta_0^2}{\lambda}(1+K_2)(K_1+K_2^2),$$

$$G_{116} = \frac{\theta_0^2}{\lambda}(1+K_1)(K_1+K_2^2), \quad G_{117} = \frac{2\theta_0^2K_1}{\lambda}(1+K_2)^2,$$

$$G_{118} = \frac{2\theta_0^2K_1}{\lambda}(1+K_1)(K_1+K_2), \quad G_{119} = \frac{\theta_0^2}{2}\left(1 - \frac{K_1^2K_2^2}{\mu\lambda}\right),$$

$$G_{120} = \frac{\theta_0^2}{2}\left(1 - \frac{K_1^3K_2}{\mu\lambda}\right), \quad G_{121} = \frac{1}{2}G_{118}, G_{122} = \frac{\theta_0^2K_1}{\lambda}(1+K_1)^2, \quad G_{123} = G_{122}.$$

$$C_{15} = -\frac{d}{ml\omega l}, \quad C_{16} = -\frac{b}{ml^2\omega_l^2\theta_0}, \quad G_{21} = \frac{1}{g\theta_0}\left(1 + \frac{K_2}{\mu\lambda^2}\right), \quad G_{22} = \frac{1}{g}\left(1 - \frac{K_1K_2}{\mu\lambda}\right),$$

$$G_{23} = \frac{1}{g}\left(1 - \frac{K_2^2}{\mu\lambda}\right), \quad G_{28} = \frac{\theta_0^2}{6}\left(1 - \frac{K_1^3K_2}{\mu\lambda}\right), \quad G_{29} = \frac{\theta_0^2}{6}\left(1 - \frac{K_2^4}{\mu\lambda}\right),$$

$$G_{210} = \frac{\theta_0^2 K_2}{\lambda}(1 + K_2)^2, \quad G_{211} = \frac{\theta_0^2}{2\lambda}(K_1 + K_2)(1 + K_2)^2,$$

$$G_{212} = \frac{\theta_0^2 K_2}{\lambda}(1 + K_1 + K_2 + K_1 K_2), \quad G_{223} = G_{221},$$

$$G_{213} = \frac{\theta_0^2}{\lambda}(K_1 + K_2)(1 + K_1 + K_2 + K_1 K_2), \quad G_{214} = \frac{\theta_0^2 K_2}{\lambda}(1 + K_1)^2, \quad G_{215} = G_{210},$$

$$G_{216} = \frac{\theta_0^2 K_2}{\lambda}(1 + K_1)(1 + K_2), \; G_{217} = 2G_{216}, \quad G_{218} = 2G_{214},$$

$$G_{219} = \frac{\theta_0^2}{2}\left(1 - \frac{K_1 K_2^3}{\mu\lambda}\right), \quad G_{220} = \frac{\theta_0^2}{2}\left(1 - \frac{K_1^2 K_2^2}{\mu\lambda}\right), \quad G_{221} = \frac{\theta_0^2}{\lambda}(1 + K_2)(K_1^2 + K_2),$$

$$G_{222} = \frac{\theta_0^2}{2\lambda}(1 + K_1)(K_1 + K_2).$$